

CHEMISTRY

A European Journal



Accepted Article

Title: Pseudo-Tetrahedral Rhodium and Iridium Complexes: Catalytic Synthesis of E-Enynes

Authors: Ana M. Geer, Alejandro Julian, José Antonio López, Miguel Ángel Ciriano, and Cristina Tejel

This manuscript has been accepted after peer review and appears as an Accepted Article online prior to editing, proofing, and formal publication of the final Version of Record (VoR). This work is currently citable by using the Digital Object Identifier (DOI) given below. The VoR will be published online in Early View as soon as possible and may be different to this Accepted Article as a result of editing. Readers should obtain the VoR from the journal website shown below when it is published to ensure accuracy of information. The authors are responsible for the content of this Accepted Article.

To be cited as: *Chem. Eur. J.* 10.1002/chem.201803878

Link to VoR: <http://dx.doi.org/10.1002/chem.201803878>

Supported by
ACES

WILEY-VCH

Pseudo-Tetrahedral Rhodium and Iridium Complexes: Catalytic Synthesis of *E*-Enynes

Ana M. Geer, Alejandro Julián, José A. López, Miguel A. Ciriano, and Cristina Tejel*

Dedicated In Memoriam to Professor Dr. Pascual Royo

Abstract: Reactions of rhodium(I) and iridium(I) complexes $[M(\text{PhBP}_3)(\text{C}_2\text{H}_4)(\text{NCMe})]$ with alkynes result in the synthesis of a new family of pseudo-tetrahedral complexes, $[M(\text{PhBP}_3)(\text{RC}\equiv\text{CR}')] (M = \text{Rh, Ir; PhBP}_3 = \text{PhB}(\text{CH}_2\text{PPh}_2)_3^-)$, which contain an alkyne as a four-electron donor. Reactions of these unusual compounds with two-electron donors ($L = \text{PMe}_3, \text{CN}^t\text{Bu}$) produces a change in the 'donicity' of the alkyne from a $4e^-$ to a $2e^-$ donor to give five-coordinate complexes. These are the final products for iridium while further reactions take place for the rhodium complexes. In particular, C(sp)-H bond activation of the alkyne leading to hydrido-alkynyl complexes occurs. This process is essential in a further reactivity of the alkynes, and thus if the alkyne itself is used as a ligand, *E*-enynes complexes are obtained. As a consequence of this chemistry, we showcase that complex $[\text{Rh}(\text{PhBP}_3)(\text{C}_2\text{H}_4)(\text{NCMe})]$ is a very efficient precatalyst for the regioselective dimerization and trimerization of terminal alkynes to *E*-enynes. Interestingly, acetonitrile significantly enhances the catalytic activity facilitating the C(sp)-H bond activation step. A hydrometallation mechanism to account for these experimental observations is proposed.

Introduction

Alkynes play a pivotal role in the synthesis of a wide range of organics derived from the high versatility of the 'C≡C' functionality. They include the well-known Sonogashira couplings,^[1] oxidative alkynylations,^[2] hydroacylations,^[3] dimerizations,^[4] redox-neutral α -amine alkynylations,^[5] metathesis,^[6] hydrogenations,^[7] hydrosilylations,^[8] hydroaminations,^[9] cycloisomerizations,^[10] as well as three-component couplings including [2+2+2] cycloadditions.^[11] Coordination of the alkyne to a metal center is often one of the initial steps in these types of transformations; therefore a fundamental knowledge of the metal-alkyne interaction is essential for the development of new processes and catalysis. Moreover, from a theoretical point of view, analysis of the bonding between an alkyne and a transition metal complex is also interesting because the ambivalent character of alkynes as ligands, behaving either as $2e^-$ or $4e^-$ donors.^[12] Accordingly,

Bianchini proposed a π -alkyne metal complex as the first step in the mechanism for alkyne cyclotrimerization when using rhodium and iridium compounds with the tripodal neutral phosphine triphos as the catalyst, and described the cationic complexes $[\text{Rh}(\text{MeCP}_3)(\text{RC}\equiv\text{CR})]\text{BPh}_4$ ($R = \text{CO}_2\text{Me, Ph; MeCP}_3 = \text{MeC}(\text{CH}_2\text{PPh}_2)_3$).^[13] Unfortunately, the lack of crystallographic studies prevented their full characterization, and they were assumed to be in a fast equilibrium in solution between trigonal-bipyramidal and square-pyramidal species on the basis of spectroscopic studies.

A survey on the literature revealed that η^2 -alkyne coordination to rhodium is dominated by a two-electron donicity stabilizing both, trigonal bipyramid (*TBPY*) and square-planar (*SP*) complexes. From the few examples crystallographically characterized, electronically saturated *TBPY* complexes are derived from metal fragments such as 'RhCl(PMe₃)₃',^[14] 'RhCp'P'Pr₃^[15] or 'RhTp(L)',^[16] while the metallic fragments 'Rh(X)(P'Pr₂)' ($X = \text{Cl, I}$)^[17] and 'Rh(acac)(olefin)'^[18] are suitable to bind alkynes to electronically unsaturated 16 eV *SP*-compounds. More recently, *SP*-complexes with functionalized alkynes like thioether-alkynylborates,^[19] and P(C≡C)P pincer type ligands^[20] have been described.

Herein we report the synthesis, full characterization, reactivity studies, and electronic structure of the neutral $[M(\text{PhBP}_3)(\text{RC}\equiv\text{CR}')] (M = \text{Rh, Ir; PhBP}_3 = \text{PhB}(\text{CH}_2\text{PPh}_2)_3^-)$ complexes with a unique pseudo-tetrahedral geometry, which give an insight into this very unusual coordination environment for mononuclear d^8 -metal complexes of the second and third row. Indeed, tetrahedral or pseudo-tetrahedral geometries are unknown in rhodium(I) chemistry so far,^[21] and they are restricted to rhodium(-I) and rhodium(0) oxidation states.^[22] Nonetheless, despite of the strong propensity of d^8 -RhL₄ complexes to adopt square-planar geometries, rare sawhorse (*SH*) environments have also been reported,^[23] while the unique compound $[\text{Rh}(\text{trop}_2\text{SiMe})(\text{C}_2\text{H}_4)]$ remains the sole example for the related trigonal pyramid (*TP*) geometry.^[24]

Moreover, we have studied the chemistry of these complexes and, as a consequence, we have uncovered that the rhodium complexes are efficient precatalysts for terminal alkyne dimerization with a high selectivity to *E*-enynes, which is a long pursued proposal. Part of this work has been previously communicated.^[25]

Results and Discussion

Synthesis and Characterization of $[M(\text{PhBP}_3)(\text{CR}\equiv\text{CR}')] (M = \text{Rh, Ir})$

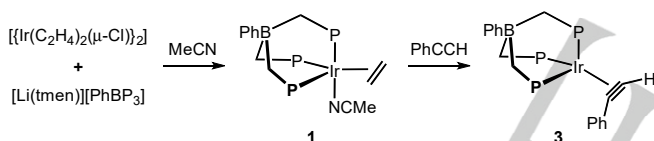
The iridium monoolefin complex $[\text{Ir}(\text{PhBP}_3)(\text{C}_2\text{H}_4)(\text{NCMe})]$ (**1**) ($\text{PhBP}_3 = [\text{PhB}(\text{CH}_2\text{PPh}_2)_3]^-$) was synthesized in order to prepare iridium alkyne complexes, since it contains two labile

[a] Dr. A. M Geer, A. Julián, Dr. J. A. López, Prof. Dr. M. A. Ciriano, Dr. C. Tejel
Departamento de Química Inorgánica
Instituto de Síntesis Química y Catálisis Homogénea-ISQCH, CSIC-
Universidad de Zaragoza
Pedro Cerbuna 12, 50009-Zaragoza (Spain)
E-mail: ctejel@unizar.es

Supporting information for this article is given via a link at the end of the document.

(acetonitrile and ethylene) ligands, as observed for the analogous rhodium complex $[\text{Rh}(\text{PhBP}_3)(\text{C}_2\text{H}_4)(\text{NCMe})]\cdot 2\text{MeCN}$ (**2**).^[26] With this purpose, $[\{\text{Ir}(\text{C}_2\text{H}_4)_2(\mu\text{-Cl})\}_2]$ was treated with 1 mol-equiv. of $[\text{Li}(\text{tmen})][\text{PhB}(\text{CH}_2\text{PPh}_2)_3]$ (tmen = N,N,N',N'-tetramethylethane-1,2-diamine) in an ethylene saturated solution of acetonitrile to provide **1**, which precipitated in the reaction medium as a pure white solid (Scheme 1). Noticeably, no activation of C–H bonds was observed in our case, in contrast to similar metathesis reactions of the phosphine with $[\{\text{Ir}(\text{coe})_2(\mu\text{-Cl})\}_2]$ (coe = cyclooctene) and $[\{\text{Ir}(\text{H}_2\text{C}=\text{CHMe})_2(\mu\text{-Cl})\}_2]$, which result in hydrideallyridium(III) complexes.^[27]

Complex **1** is pentacoordinate with a trigonal bipyramidal geometry (*TBPY*), analogous to the rhodium complex **2**, but they differ in that the ^1H and $^{31}\text{P}\{^1\text{H}\}$ NMR spectra of the iridium complex correspond to a static species. Thus, according to the proposed structure, the $^{31}\text{P}\{^1\text{H}\}$ NMR spectrum displays a doublet for the two equivalent equatorial phosphorus nuclei and a triplet for the axial phosphorus atom. The C=C bond of the coordinated ethylene is located within the equatorial plane and it does not rotate, as evidenced by two distinct signals in the ^1H NMR spectrum due to the protons on both sides of the equatorial plane. The lack of rotation of ethylene is a consequence of a strong metal-olefin π -interaction, which occurs at the equatorial position for *TBPY* $d^8\text{-ML}_5$ complexes.^[28] In sharp contrast, the ethylene in the rhodium counterpart **2** displays free rotation at r.t., suggesting thus that ethylene is more tightly bound to iridium than rhodium.



Scheme 1. Synthesis of complexes **1** and **3**.

Reactions of phenylacetylene, propargyl alcohol and methyl propiolate with complex **1** in toluene were easily detected by a color change of the solution from colorless to orange at room temperature. They proceed with the corresponding replacement of both the ethylene and acetonitrile ligands by the alkyne to yield the corresponding complexes $[\text{Ir}(\text{PhBP}_3)(\text{HC}=\text{CR})]$ ($\text{R} = \text{Ph}$, **3**; CH_2OH , **4**; CO_2Me , **5**) (Scheme 1). However, no reaction was observed with the internal alkyne dimethylacetylenedicarboxylate (dmad). Noticeably, the replacement of two 2-e^- ligands by one triple C \equiv C bond is a first clear indication that the alkyne behaves as a four-electron ligand. Complexes **3-4** were isolated as orange crystalline solids in good yields and were fully characterized while complex **5** was characterized *in situ*. In addition, the structure of **3** was determined by X-ray diffraction methods. An ORTEP diagram of the complex is shown in Figure 1.

The geometry around the iridium atom was found to be pseudo-tetrahedral with the iridium center bound to the three phosphorus atoms of the PhBP_3 ligand and to the C \equiv C bond of

phenylacetylene in a η^2 fashion. The short iridium–carbon and long C46–C47 bond distances (2.001 Å in average and 1.32 Å, respectively) of the η^2 coordinated alkyne are consistent with the alkyne acting as a four-electron donor in **3**.^[12a,29] Also the C \equiv C–C angle is considerably bent up to 137° . The three P–Ir–Ct angles (Ct is the middle point of the C \equiv C bond) were found to be different while the topology of the tripodal ligand impose P–Ir–P angles close to 90° .^[30]

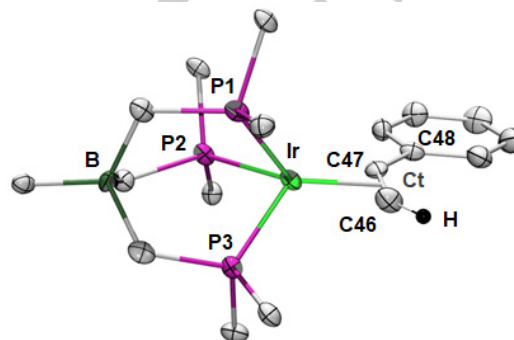


Figure 1. Structure (ORTEP at 50% level) of the complex, $[\text{Ir}(\text{PhBP}_3)(\text{HC}=\text{CPh})]$ (**3**). Hydrogen atoms have been omitted and only the C^{ipso} atoms of the phenyl groups from PhBP_3 are shown for clarity. Selected angles ($^\circ$) and bond distances (Å) for complex **3**: Ir–P1, 2.242(2); Ir–P2, 2.334(2); Ir–P3, 2.280(2); Ir–C46, 1.979(8); Ir–C47, 2.019(8); Ir–Ct, 1.888(8); C46–C47, 1.318(10); C47–C48, 1.464(10); P1–Ir–Ct, 129.1(2); P2–Ir–Ct, 127.8(2); P3–Ir–Ct, 123.4(2); C46–C47–C48, 137.1(8). (Ct is the middle point between C46 and C47).

Additionally, the three Ir–P bond distances are unequal. Assuming that the C \equiv C bond occupies one coordination position, the 'Ir(PhBP_3)' fragment possesses a local symmetry slightly distorted from C_{3v} , in which the atoms of boron and iridium would define the C_3 axis. In this structure, Ct is somewhat shifted from the C_{3v} axis (axis(B,Ir)–Ct, $176.78(2)^\circ$). This off-axis distortion makes the P2–Ir–Ct angle smaller than the other two P–Ir–Ct angles. These structural features are very similar to those found for one independent molecule in the crystal and in the DFT calculated structures of the analogous rhodium complex $[\text{Rh}(\text{PhBP}_3)(\text{HC}=\text{CPh})]$ (**6**),^[25] although the C \equiv C bond distance is longer for iridium as a consequence of a stronger π -back donation.

There are only two η^2 -alkyne-iridium(I) tetracoordinated complexes characterized crystallographically: $[\text{Ir}(\text{PMe}_2\text{Ph})_3(\text{MeC}=\text{CMe})]\text{BF}_4$, described by Caulton^[31] as roughly square-pyramidal with the alkyne acting as a four-electron donor and $[\text{Ir}(\text{COCH}_2\text{Me}_3)(\text{P}(p\text{-tolyl})_3)_2(\text{MeO}_2\text{CC}=\text{CCO}_2\text{Me})]$, with a distorted tetrahedral geometry, where the authors propose that the alkyne is a two-electron donor considering the lack of signals for the multiple-bonded carbon atoms.^[32] However, both complexes possess similar geometrical features to those of **3**. Consequently, these three species can be described as 18-electron complexes with a pseudo-tetrahedral geometry, which is very uncommon for rhodium(I) and iridium(I) compounds. Some fluxional *fac*-triphosphorodiridium and -iridium complexes with alkynes reported by

Bianchini can also be included into this category on the basis of spectroscopic studies.^[13]

Treatment of the rhodium complex $[\text{Rh}(\text{PhBP}_3)(\text{C}_2\text{H}_4)(\text{NCMe})]\cdot 2\text{MeCN}$ (**2**) in toluene with terminal and internal alkynes gave directly the complexes $[\text{Rh}(\text{PhBP}_3)(\text{RC}\equiv\text{CR}')] (R = \text{H}; R' = \text{Ph}$ (**6**), *p*- MeC_6H_4 (**7**), *p*- tBuC_6H_4 (**8**), $\text{}^n\text{Bu}$ (**9**), CH_2OH (**10**), CO_2Me (**11**); $R = R' = \text{CO}_2\text{Me}$, **12**), which were isolated as reddish-brown solids after work up. The reaction is similar to the above described for the iridium complex **1** and it is clearly detected by a color change of the solution from yellow to red-brown.

The spectroscopic data of the iridium and rhodium complexes are comparable (Table 1) to those reported for the complex $[\text{Rh}(\text{PhBP}_3)(\text{HC}\equiv\text{CPh})]$ (**6**). Thus, compounds **3–12** show equivalent phosphorus nuclei and give a singlet (Ir) or doublet (Rh) in the $^{31}\text{P}\{^1\text{H}\}$ NMR spectra even at low temperature. This feature requires a fast rotation of the alkyne around the M–Ct axis, which has a very low energy barrier as calculated for the rhodium complex **6** (ca. 1 kcal mol⁻¹).^[25] The facile rotation of the alkyne results from an almost continuous overlap of the orbitals involved in the metal–alkyne bond along the axis of rotation, thus avoiding a bond cleavage.

Aside from the equivalence of the phosphorus nuclei, other noticeable spectroscopic characteristics of these compounds are the large shift to low-field of the proton of the terminal alkynes in the ^1H NMR spectra as well as the signals of the bound acetylene carbons ca. 160 ppm in the $^{13}\text{C}\{^1\text{H}\}$ NMR spectra. Both features are typical for alkynes behaving as four-electron donors.^[12b-d]

Table 1. Selected NMR spectroscopic data (δ (ppm)) for complexes $[\text{M}(\text{PhBP}_3)(\text{RC}\equiv\text{CR}')] (M = \text{Rh}, \text{Ir})$.

Complex	^1H (HC \equiv)	$^{13}\text{C}\{^1\text{H}\}$ (RC \equiv , $\equiv\text{CH}$)	$^{31}\text{P}\{^1\text{H}\}$
3	11.77 (q)	179.8, 166.3	14.6 (s)
4	10.91 (qt)	182.2, 157.8	16.5 (s)
5	11.08 (q)	167.1, 164.8	17.7 (s)
6	10.04 (qd)	164.9, 151.8	47.7 (d)
7	10.11 (qd)	165.0, 152.2	47.2 (d)
8	10.18 (qd)	164.9, 152.4	47.6 (d)
9	9.52 (qd)	167.7, 144.8	47.6 (d)
10	9.36 (qd)	166.4, 144.1	48.6 (d)
11	9.46 (q)	154.0, 148.4	51.6 (d)
12	-	152.7	53.1 (d)

A common and noticeable characteristic of all reactions is that neither ethylene nor acetonitrile remain coordinated to the metal. Indeed, complexes of the type $[\text{M}(\text{PhBP}_3)(\text{RC}\equiv\text{CR}')(L)] (L = \text{C}_2\text{H}_4 \text{ or } \text{MeCN})$ have not been observed. With this in mind it is

mentionable that the rhodium complex **2** reacts with styrene to give $[\text{Rh}(\text{PhBP}_3)(\text{H}_2\text{C}=\text{CHPh})(\text{NCMe})]$ (**13**), with an axial acetonitrile ligand (see Experimental Section). Since the styrene complex **13** and the hypothetical compound $[\text{Rh}(\text{PhBP}_3)(\text{HC}\equiv\text{CPh})(\text{NCMe})]$ (**A**) only differ in two protons, steric effects are not the origin for the formation of the tetracoordinate $[\text{Rh}(\text{PhBP}_3)(\text{HC}\equiv\text{CPh})]$ (**6**). Consequently, electronic effects arising from the change of the 'donicity' of the alkyne (from 2 to 4 e⁻) along with the entropy change associated to acetonitrile dissociation (on going from **A** to **6**) seems to be the main factors that govern the result of this reaction.

In theory, tetrahedral complexes of Rh(I) and Ir(I) should be paramagnetic with two unpaired electrons according to the classical d-orbital splitting. However, on decreasing the T_d symmetry to C_{3v} by closing three angles, the d^2 -based orbital is lowered in energy while a low-energy hybrid sp orbital ($2a_1$) becomes available for bonding.

DFT analysis of the $d^8\text{-M}\{\text{MeB}(\text{CH}_2\text{PMe}_2)_3\}$ ($M = \text{Rh}, \text{Ir}$) fragments indicates a small difference in energy in favor of the triplet versus the singlet state (3.0 and 2.0 kcal mol⁻¹ for Rh and Ir, respectively). However, this difference can be meaningless because of the tendency of the B3LYP functional to stabilize high-spin species.^[33] Consequences of the spin-pairing are: a) a distortion of the framework that results in distinct M–P bond distances and P–M–P bond angles that reduces the symmetry from C_3 (triplet) to Cs (singlet); b) a drastic energy difference (2.36 and 2.13 eV for Rh and Ir, respectively) between the HOMO ($2e_a$) and LUMO ($2e_s$) that stabilizes the singlet state and leaves empty the orbital $2e_s$ of parentage d_{yz} .

The two empty frontier orbitals ($2a_1$, and $2e_s$) in the singlet state of the $d^8\text{-M}\{\text{MeB}(\text{CH}_2\text{PMe}_2)_3\}$ fragment match those filled $\pi_{||}$ and π_{\perp} orbitals of the bent C \equiv C bond. They form thus two bonding MOs, namely σ and π , which are filled with four electrons given by the alkyne, stabilizing a pseudo-tetrahedral geometry for an 18 electron complex. A further match of the filled $2e_a$ orbital with the empty $\pi_{||}^*$ orbital of the C \equiv C bond corresponds to a π -backdonation.^[25] This picture supports a mayor contribution of the pseudo-tetrahedral M(I)–alkyne canonical form. The alternative pseudo-square-pyramidal M(III)–metallacyclopentene description could be also considered to give account for the proton and carbon low-field shifts. However, the equivalence of the three P atoms in the $^{31}\text{P}\{^1\text{H}\}$ NMR spectra would require an easy P-donor exchange through either trigonal bipyramidal structures or P–M bond dissociation, which in our experience for Rh(III) and Ir(III) complexes involve energy barriers quite larger than that calculated (1 kcal mol⁻¹).^[34]

The DFT-computed optimized geometries of the model complexes $[\text{M}\{\text{MeB}(\text{CH}_2\text{PMe}_2)_3\}(\text{HC}\equiv\text{CPh})]$ ($M = \text{Ir}, \mathbf{3}'$; $\text{Rh}, \mathbf{6}'$) as closed-shell species reproduce quite well the experimental data found for **3** and **6**. In particular, the agreement of the M–P bond distances and P–M–P bond angles with the experimental data is remarkable. This geometric irregularity characteristic of the metallic fragments $d^8\text{-M}\{\text{MeB}(\text{CH}_2\text{PMe}_2)_3\}$ in the singlet state is retained in the complexes while the HOMO–LUMO gap increases to 3.48 and 3.81 eV in **6'** and **3'**, respectively. The representations and composition of the MOs of the model

complexes show strong mixing, therefore a direct comparison with the MOs of the fragment is difficult.

Reactions of complexes $[M(\text{PhBP}_3)(\text{HC}\equiv\text{CPh})]$ with two-electron donor ligands.

Reactivity studies on these novel complexes was initiated with $[M(\text{PhBP}_3)(\text{HC}\equiv\text{CPh})]$ ($M = \text{Ir}$, **3**; Rh , **6**). Although they are electronically saturated (18 electron), both compounds present a low-lying energy LUMO pointing out towards a possible vacant site (Figure 2).

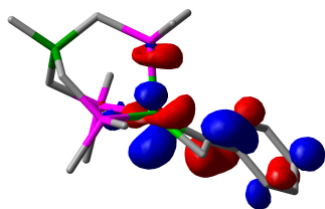
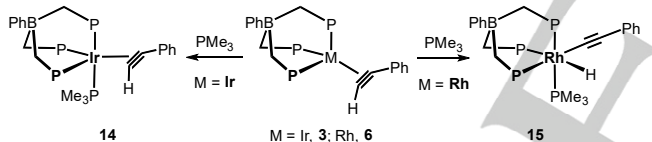


Figure 2. LUMO of complex $[\text{Ir}(\text{MeB}(\text{CH}_2\text{PMe}_2)_3)(\text{HC}\equiv\text{CPh})]$ (**3'**).

Thus, good σ -donor ligands such as PMe_3 react with **3** and **6** to give $[\text{Ir}(\text{PhBP}_3)(\text{HC}\equiv\text{CPh})(\text{PMe}_3)]$ (**14**) and $[\text{Rh}(\text{PhBP}_3)(\text{C}\equiv\text{CPh})(\text{H})(\text{PMe}_3)]$ (**15**) in very high yields (Scheme 2). There is a notable influence of the metal center on the products obtained, yielding a pentacoordinate complex for iridium but a hydrido alkynyl compound for rhodium.



Scheme 2. Synthesis of complexes **14** and **15** from reactions of PMe_3 with **3** and **6**, respectively.

The most significant spectroscopic features observed for **14** are the chemical shifts of the acetylenic proton and carbon atoms, which are substantially shifted towards higher field relative to **3** (Table 2). These shifts indicate a clear change in the 'donicity' of the phenylacetylene from a 4-electron donor (in **3**) to a 2-electron donor (in **14**). The result contrasts with that obtained for the rhodium species **6**, where addition of PMe_3 enables a $\text{C}(\text{sp})\text{-H}$ bond activation reaction to give the hydrido alkynyl complex $[\text{Rh}(\text{PhBP}_3)(\text{C}\equiv\text{CPh})(\text{H})(\text{PMe}_3)]$ (**15**) (Scheme 2). Relevant signals for **15** corresponds to the hydride ligand ($\delta = -8.74$ ppm, dddt) and to the acetylide carbon atoms ($\delta = 111.5$ ($\equiv\text{CPh}$), 109.5 ppm ($\text{RhC}\equiv$)) in the ^1H and $^1\text{H}, ^{13}\text{C}$ -hmbc NMR spectra, respectively. The expected ABCMX spin system ($M = \text{PMe}_3$, $X = ^{103}\text{Rh}$) is clearly observable in the $^{31}\text{P}\{^1\text{H}\}$ NMR spectrum (see Supporting Information). Formation of the rhodium-hydrido-alkynyl complex most likely involves the pentacoordinated intermediate, $[\text{Rh}(\text{PhBP}_3)(\text{HC}\equiv\text{CPh})(\text{PMe}_3)]$

(**B**), analogous to the iridium counterpart **14**. However, this species was not detected even monitoring the reaction at -70 °C.

Further evidence for the participation of η^2 -alkyne pentacoordinated intermediates in the C–H bond activation process was obtained from the reaction of **6** with $^t\text{BuNC}$, a slightly weaker donating ligand than PMe_3 ,^[35] which allowed the detection of the intermediate $[\text{Rh}(\text{PhBP}_3)(\text{HC}\equiv\text{CPh})(\text{CN}^t\text{Bu})]$ (**16**) by ^1H and $^{31}\text{P}\{^1\text{H}\}$ NMR spectroscopy at -50 °C. However, the complex evolves very quickly to $[\text{Rh}(\text{PhBP}_3)(\text{C}\equiv\text{CPh})(\text{H})(\text{CN}^t\text{Bu})]$ (**17**) on raising the temperature. Selected spectroscopic data of **16** and **17** can be found in Table 2 and are in agreement with the proposed formulation.

Table 2. Selected NMR spectroscopic data (δ (ppm)) for complexes **14–21**.^[a]

Complex	^1H ($\text{HC}\equiv$ / Rh-H)	$^{13}\text{C}\{^1\text{H}\}$ ($\text{RC}\equiv$, $\equiv\text{CH}$)	$^{31}\text{P}\{^1\text{H}\}$
3	11.77 (q)	179.8, 166.3	14.6 (s)
6	10.04 (qd)	164.9, 151.8	47.7 (d)
14	6.13 (t)	89.0, 83.1	-7.7, -17.8, -39.6, -47.6
15	-8.74 (ddt)	111.5, 109.5	28.4, 21.1, 4.7, -11.6
16	5.97 (dd)	- ^[b] , 84.6	25.5, 22.2, 15.1
17	-7.19 (ddt)	110.6, 103.4	28.9, 25.8, 4.3
18	6.80 (t)	111.3, 87.9	22.0, 18.0, 12.8, -11.2
19	-8.74 (ddt)	- ^[b] , - ^[b]	27.4, 19.7, 5.4, -11.6
20	–	167.4, 161.8	45.8 (d)
21	–	168.1, 163.3	45.2 (d)

[a] The pseudrotetrahedral complexes **3** and **6** have also been included for comparative purposes. [b] Not detected.

Although a decrease of the electronic density at the metal slightly slows down the C–H oxidative addition reaction, releasing electronic density in the alkyne showed a more noticeable effect. Thus, addition of PMe_3 to the complex which contains the electron acceptor alkyne $[\text{Rh}(\text{PhBP}_3)(\text{HC}\equiv\text{CCO}_2\text{Me})]$ (**11**) allowed the isolation of $[\text{Rh}(\text{PhBP}_3)(\text{HC}\equiv\text{CCO}_2\text{Me})(\text{PMe}_3)]$ (**18**) as an orange solid in excellent yields. Spectroscopic data of **18** confirm the presence of the alkyne as a two-electron donor (Table 2). This complex slowly transforms in solution into the corresponding hydrido alkynyl derivative $[\text{Rh}(\text{PhBP}_3)(\text{C}\equiv\text{CCO}_2\text{Me})(\text{H})(\text{PMe}_3)]$ (**19**) quantitatively, but this reaction requires one week at room temperature to reach completion. From these solutions complex **19** was isolated as colorless microcrystals whose molecular structure is depicted in Figure 3.

In **19**, the rhodium atom is bound to four phosphorus atoms (PMe_3 and the three from the $[\text{PhBP}_3]$), the hydrido, and the alkynyl ligand through a σ -Rh–C bond in a slightly distorted octahedral geometry. The strong *trans* influence of the hydrido ligand is clearly reflected in a longer Rh–P2 bond distance (*trans*

to it) when compared with the other three that are almost equal. The methylcarboxylate group (CO₂Me) was found to be disordered over two positions (only one of them, labelled with the letter 'a' with a relative occupancy' of 85.2(7)% is shown in Figure 3). The C49–C50 bond distance falls in the range for terminal alkynyl ligands and is practically linear, with Rh–C49–C50 and Rh–C49–C51a/b angles close to 180°.

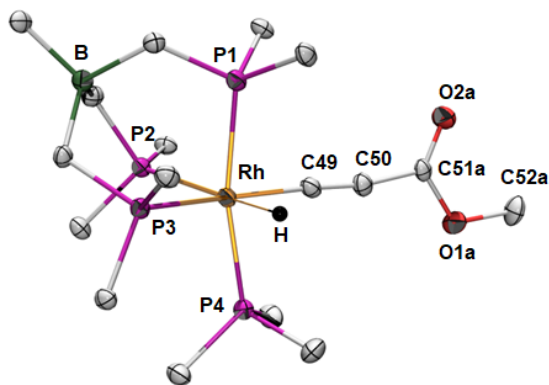


Figure 3. Structure (ORTEP at 50% level) of [Rh(PhBP₃)(C≡CCO₂Me)(H)(PMe₃)] (**19**). Hydrogen atoms have been omitted and only the C^{ipso} atoms of the phenyl groups from PhBP₃ are shown for clarity. Selected angles (°) and bond distances (Å): Rh–P1, 2.367(1); Rh–P2, 2.460(1); Rh–P3, 2.355(1); Rh–P4, 2.345(1); Rh–C49, 2.017(4); C49–C50, 1.212(5); C50–C51a, 1.438(5); C50–C51b, 1.440(7); P1–Rh–P4, 167.4(4); P2–Rh–H, 174(2); P3–Rh–C49, 166.0(1).

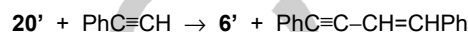
Reactions leading to complexes **14–19** indicate that subtle changes in both, the substituent on the alkyne ligand or the two-electron ligand (L = PMe₃, CN^tBu) on the metal can result in significant differences in reactivity for rhodium. Moreover, the most surprising difference is the lack of C–H bond activation for the iridium complex **14** since this metal is thought to be more suitable for this type of reactions than rhodium.^[36] In our opinion, this lack of reactivity of the iridium complex **3** can be mainly attributed to kinetic reasons. In addition, it is also noticeable the long reaction time for the C–H bond activation in [Rh(PhBP₃)(HC≡CCO₂Me)(PMe₃)] (**18**), with an electron withdrawing group on the alkyne.

Interestingly, if the alkyne itself is used as a ligand, *E*-enyne complexes are obtained. In this manner, the reaction of [Rh(PhBP₃)(C₂H₄)(NCMe)]·2MeCN (**2**) with two mol-equiv. of phenylacetylene gives the complex [Rh(PhBP₃)(PhC≡C–CH=CHPh)] (**20**), while a similar reaction with *p*-tolylacetylene gives [Rh(PhBP₃)(*p*-tolC≡C–CH=CH*p*)] (**21**). Complexes **20** and **21** represent two new examples of rhodium(I) species in a pseudotetrahedral geometry with the triple C≡C bond bound to the metal. They were isolated as dark red solids fully characterized by analytical and spectroscopic methods according to the formulation shown in Figure 4.

Remarkably, both reactions were found to be regioselective, observing the formation of the *E* isomer, as indicated by the large coupling constant of the olefinic protons (³*J*(H,H) = 15.7–15.9 Hz). On the contrary, no further reaction was observed

between [Ir(PhBP₃)(HC≡CPh)] (**3**) and phenylacetylene, even when added in excess.

DFT calculations on the model complex [Rh(MeBP₃)(PhC≡C–CH=CHPh)] (**20'**, MeBP₃ = MeB(CH₂PMe₂)₃) confirm the proposed structure (Figure 4, right). Noticeably, rhodium retains the pseudotetrahedral geometry even in the presence of the close C=C bond. These calculations also indicate that from a thermodynamic perspective, a value of Δ*G*₂₉₈^o = –0.4 kcal mol^{–1} is obtained for the alkyne exchange reaction:



Therefore, substitution of the enyne by phenylacetylene is possible, closing thus a plausible catalytic cycle for the dimerization of phenylacetylene. Indeed, preliminary assays indicated the reaction to be catalytic.

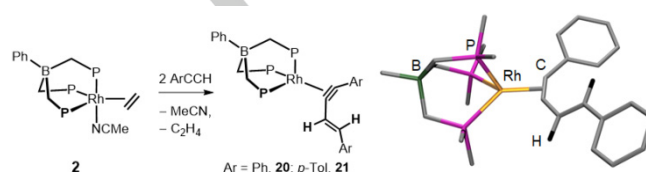


Figure 4. Left: synthesis of the *E*-enyne complexes **20** and **21**. Right: DFT calculated structure for the model complex [Rh(MeBP₃)(PhC≡C–CH=CHPh)] (**20'**, MeBP₃ = MeB(CH₂PMe₂)₃).

Catalytic synthesis of enynes.

A first test for the dimerization of phenylacetylene by using [Rh(PhBP₃)(HC≡CPh)] (**6**) (in a 5 mol% catalyst loading) resulted in the conversion to the corresponding enyne (1,4-diphenyl-but-3-en-1-yne) with good regioselectivity to the *E* isomer (Table 3, entry 1). However, the reaction was found to be very slow. Remarkably, we found that the reaction time can be significantly reduced if the rhodium(I) derivative **2** was used as a catalyst precursor (entry 2). A comparison of both reactions by NMR spectroscopy indicated that the only difference is the presence of free acetonitrile in the reaction media when using **2** as precatalyst, since this complex crystallizes with two molecules of acetonitrile. Therefore, acetonitrile was responsible for the increase in catalytic activity. Indeed, if the catalysis was carried out in the presence of 10 equivalents of acetonitrile (per mol of **2**), the time of the reaction was reduced to 40 min (entry 3). Moreover, if the catalysis is performed in neat acetonitrile the quantitative conversion of the phenylacetylene is considerably reduced (15 min) even at 60 °C, maintaining the regioselectivity to the *E* isomer (entry 4) (Figure 5). Nonetheless, lowering the temperature to r.t. increased the reaction time considerably (entry 5).

The catalysts work equally well with a wider variety of alkynes, such as the aryl *p*-tolC≡CH, the functionalized Me₃SiC≡CH or the alkylic ⁿBuC≡CH. Using complex **2** as precatalyst in neat acetonitrile at 60 °C, the corresponding enynes were obtained with a high selectivity to the *E* isomers and with short reaction times (Table 3, entries 6–8). Under these conditions complex **2** is one of the fastest catalysts reported so far with the advantage that no additives are necessary.^[37]

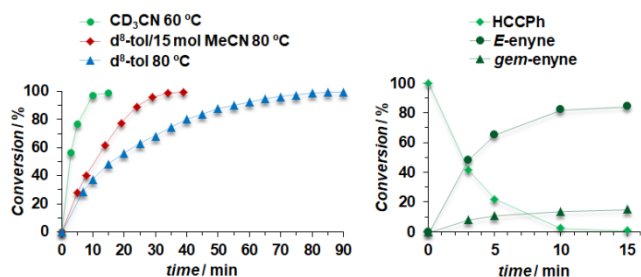


Figure 5. Left: Conversion (%) vs time for the synthesis of PhC≡C-CH=CHPh (*E*+*gem*) using complex **2** as precatalyst showing the beneficial effect of acetonitrile. Right: Details of this reaction in neat CD₃CN at 60 °C.

The results of lowering the catalyst loading to 1 mol%, (entries 9-12) have been also included in Table 3 for comparative purposes. Good reaction times (11-82 min) are still maintained and similar high selectivities towards the *E*-enyne are again obtained.^[38]

Table 3. Catalytic dimerization of alkynes to enynes mediated by complexes **6** or **2**.^[a]

Entry	Alkyne	Cat (mol%)	T (°C) / Solvent	Time	% Convers. (<i>E/gem</i>) ^[b]
1	PhC≡CH	6 (5)	80 / [D ₈]tol	30 h	> 99 (85:15)
2	PhC≡CH	2 (5)	80 / [D ₈]tol	90 min	> 99 (82:18)
3	PhC≡CH	2 (5)	80 / [D ₈]tol: CD ₃ CN ^[c]	40 min	> 99 (83:17)
4	PhC≡CH	2 (5)	60 / CD ₃ CN	15 min	> 99 (85:15)
5	PhC≡CH	2 (5)	25 / CD ₃ CN	9 h	> 99 (83:17)
6	<i>p</i> -tolC≡CH	2 (5)	60 / CD ₃ CN	10 min	> 99 (84:16)
7	Me ₃ SiC≡CH	2 (5)	60 / CD ₃ CN	4 min ^[d]	> 99 (95:5)
8	ⁿ BuC≡CH	2 (5)	60 / CD ₃ CN	10 min	> 99 (88:12)
9	PhC≡CH	2 (1)	60 / CD ₃ CN	82 min	> 99 (85:15)
10	<i>p</i> -tolC≡CH	2 (1)	60 / CD ₃ CN	58 min	> 99 (84:16)
11	Me ₃ SiC≡CH	2 (1)	60 / CD ₃ CN	11 min	> 99 (95:5)
12	ⁿ BuC≡CH	2 (1)	60 / CD ₃ CN	52 min	> 99 (86:14)
13	PhC≡CH	2 (0.1)	60 / CD ₃ CN	15 h	68 (85:15)
14	Me ₃ SiC≡CH	2 (0.1)	60 / CD ₃ CN	72 min	> 99 (95:5)

[a] Reaction conditions: 0.5 mL of solvent. [b] Determined by ¹H NMR spectroscopy. [c] 10 mol of CD₃CN per mol of **2**. [d] Minimum time required for lock and shim optimization.

It is interesting to mention that the reactions using the bulkiest and most electron-donating alkyne Me₃SiC≡CH (entries 7 and 11) displayed the greatest activity along with the best

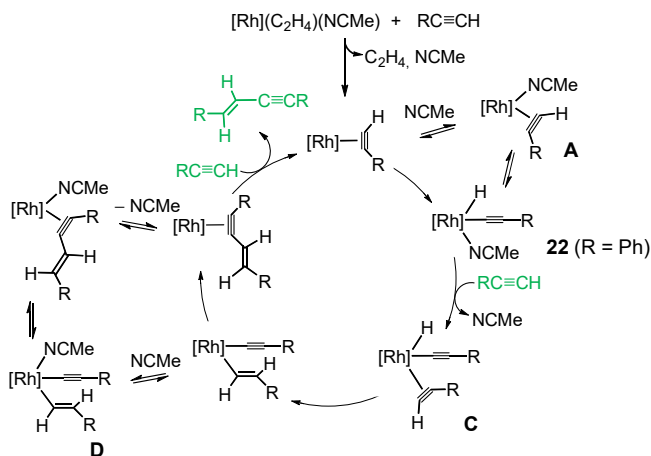
selectivities to the *E* isomer (up to 95 %). In fact, when using this alkyne the catalyst loading can be lowered to 0.1 % in a reaction which is completed in 72 min (entry 14).

As commented before, such short reaction times in alkyne dimerization are quite unusual; other known rhodium catalysts, [RhCl(IPr)(η²-coe)(py)]/py (IPr = 1,3-bis(2,6-diisopropylphenyl)imidazol-2-ylidene, py = pyridine),^[39] [Rh(POCOPⁱPr)SⁱPr₂],^[38] [Rh(PNP)(H)₂],^[40] [RhCl(PR₃)₃] (R = Ph,^[41] Me,^[42]), [Rh(η³-C₃H₅)(PⁱPr₃)₂],^[43] and [Rh(CNC-Me)(C₂H₄)] [BARF₄]^[44] require longer reaction times (3-24 h) under comparable reaction conditions to those described here. Reaction times are in general longer for other metal catalysts.^[45] Nevertheless, the use of microwave radiation has permitted a remarkable improvement in the activity of a palladium catalyst, obtaining high yields after 30 min, but with harsher reactions conditions (130 °C and addition of an external base).^[46] More recently, an iron(II) polyhydride catalyst, [Fe(PNP)(H)₂(η²-H₂)] (PNP = 2,6-di(diphenylphosphanyl-methylamine)pyridine), has been reported to promote efficiently alkyne dimerization to enynes in comparable times.^[47] In addition, selective and very fast cross-dimerization of alkynes to 1,3-enynes catalyzed by titanium complexes has been also reported.^[48] Our attempts to produce cross-dimerization of alkynes to 1,3-enynes were fully unselective resulting in a mixture of the three possible *E*-enynes.

Two main mechanistic pathways are recognized for alkyne dimerization.^{[39],[45e],[45f],[49]} The first one involves oxidative addition of the C-H bond generating a rhodium-alkynyl-hydride complex, followed by coordination of a second alkyne and either insertion of the coordinated alkyne into the M-H bond (hydrometallation) or into the M-C bond (carbometallation) and subsequent reductive elimination to afford the enyne. The second alternative involves the isomerization of the alkynyl-hydride species to the corresponding vinylidene isomer. This vinylidene mechanism leads to *E/Z* isomers while the hydro- or carbometallation paths generate *E* or *gem* enynes. Since the *Z* isomer is absent in all of the reported experiments here, catalysis with complex **2** as precatalyst most likely takes place via insertion reactions.

A plausible mechanism for alkyne dimerization using complex **2** as catalyst precursor is shown in Scheme 3. Only the hydrometallation path has been considered since this step is typically lower in energy than the carbometallation.^{[39],[45e],[45f],[49b]}

The beneficial effect of acetonitrile has also been taken into account in the C(sp)-H bond activation and the reductive-elimination steps, through species **A** and **D**, respectively (Scheme 3). Experimental evidence for the positive role of acetonitrile in the first one arises from the observation of the intermediate [Rh(PhBP₃)(H)(C≡CPh)(NCMe)] (**22**, Scheme 3) after dissolving complex [Rh(PhBP₃)(HC≡CPh)] (**6**) in neat CD₃CN, while no reaction was observed in neat C₆D₆.



Scheme 3. Plausible catalytic cycle for the synthesis of enynes catalyzed by complex **2**. A different orientation of the π -alkyne in species **C** would give the *gem* isomer. [Rh] = 'Rh(PhBP₃)'.

Moreover, DFT-calculations of intermediates **I1** and **I2**, previous to the cleavage of the C–H bond, revealed that **I2** with coordinated MeCN is 8.6 kcal mol⁻¹ lower in energy than the related **I1** without MeCN (Figure 6). Since a change in the coordination-mode of the alkyne from Rh-(η^2)C≡C to Rh-(η^2)C–H is required to achieve intermediates **I1** or **I2**, this is reasonably easier in [Rh(PhBP₃)(HC≡CR)(NCMe)] (**A**, Scheme 3) –with the alkyne acting as two-electron donor– than in [Rh(PhBP₃)(HC≡CPh)] (**6**) where it is tightly bound because of the four-electron donicity. In addition, the observed selectivity towards the *E*-isomers can be easily understood considering the steric overcrowding provided by the [PhBP₃]⁻ ligand in intermediates of type **C** in Scheme 3.

On the other hand, the iridium complex [Ir(PhBP₃)(HC≡CPh)] (**3**) is not catalytically active for this reaction, most probably due to its reluctance to undergo the C–H bond activation reaction as commented before.

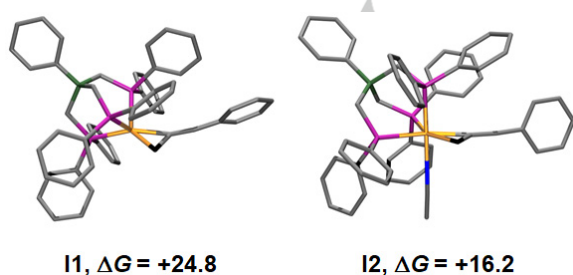


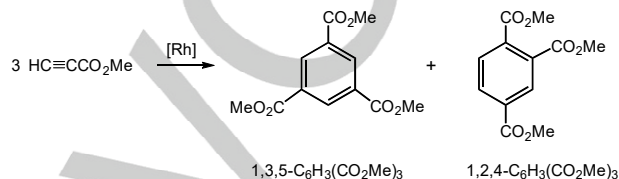
Figure 6 Calculated (DFT) molecular structures for intermediates **I1** and **I2**. Values of ΔG°_{298} are given in kcal mol⁻¹ and relative to [Rh(PhBP₃)(HC≡CPh)] (**6**) and [Rh(PhBP₃)(HC≡CPh)] (**6**) + NCMe, respectively.

Furthermore, the rhodium compound [Rh(PhBP₃)(HC≡CCO₂Me)] (**11**), for which the C–H bond activation process is slow, is also inactive for the dimerization of

the alkyne to the corresponding enyne. However, it was found to be a good catalyst for the [2+2+2] cycloaddition reaction of methyl propiolate to tri(carboxymethyl)benzene (Scheme 4).

Catalytic synthesis of trisubstituted benzenes.

Complex **2** was also found to be an appropriate precatalyst for the synthesis of trisubstituted benzenes. Scheme 4 and Table 4 summarize the results obtained for this reaction under several reaction conditions. In all the cases the reaction is almost quantitative with a good regioselectivity towards the 1,3,5-isomer relative to the 1,2,4-isomer.



Scheme 4. Cyclotrimerization of methyl propiolate catalyzed by complexes **2** and **11**.

The reaction is thermally activated as deduced from comparison of entries 1 and 2, which demonstrate considerable acceleration of the reaction on raising temperature from 25 to 80 °C. No appreciable changes were observed when using complex **11** as catalyst (entries 2 and 3). More remarkable, and in clear contrast to the dimerization of alkynes commented before, is that the presence of acetonitrile in the reaction media only slightly enhances the activity of the catalysis in the cyclotrimerization process (entry 4). This observation strongly supports a catalytic cycle in which the oxidative-addition reaction of the C–H bond is not involved. Internal activated alkynes such as MeO₂CC≡CCO₂Me did not trimerize if complexes **2**, **6** and **11** were used as catalyst precursors.

Table 4. Catalytic cyclotrimerization of methyl propiolate (HC≡CCO₂Me) mediated by **2** or **11**.^[a]

Entry	Cat.	T (°C) / Solvent	Time	% Conver. (1,3,5:1,2,4) ^[b]
1	2	25 / [D ₈]tol	12 h	98 (86:14)
2	2	80 / [D ₈]tol	16 min	> 99 (82:18)
3	11	80 / [D ₈]tol	21 min	> 99 (83:17)
4	11	80 / [D ₈]tol: CD ₃ CN ^[c]	13 min	> 99 (83:17)
5	11	60 / CD ₃ CN	55 min	> 99 (82:18)

[a] Reaction conditions: 5% Catalyst load, 0.8 M substrate, 0.5 mL of solvent. [b] Determined by ¹H NMR spectroscopy. [c] 15 mol per mol of **2**.

For this type of [2+2+2] cycloadditions, the most accepted mechanism implies the coordination of two alkyne molecules,^[50] which would lead to an intermediate species, $[\text{Rh}(\text{PhBP}_3)(\text{HC}\equiv\text{CCO}_2\text{Me})_2]$. Oxidative coupling of the two alkynes to form a metallacyclopentadiene followed by subsequent coordination of a third alkyne and its insertion into the Rh–C bond to form either a rhodacycloheptatriene (Schore's mechanism^[51]) or give an intramolecular [4+2] cycloaddition to render a 7-rhodanorbornadiene.^[52] In both cases a reductive elimination would lead to the corresponding arene.

Summary and Conclusions

In summary, we have synthesized a family of rhodium and iridium pseudo-tetrahedral alkyne complexes of formula $[\text{M}(\text{PhBP}_3)(\text{HC}\equiv\text{CR})]$ (M = Ir, Rh), in which the alkyne ligand behaves as a four-electron donor. This unique coordination environment is achievable by the combination of a strongly donating and strong-field tripodal $[\text{PhBP}_3]^-$ ligand with alkyne ligands acting as four electron donors. Further reactions of these compounds with two-electron donor ligands (L = *t*BuNC and PMe_3) lead to noticeably contrasting reactivity depending on the metal. For rhodium, the hydrido alkynyl complexes $[\text{Rh}(\text{PhBP}_3)(\text{C}\equiv\text{CR})(\text{H})\text{L}]$ are the final result from these reactions. These compounds are formed through a C–H bond activation in the terminal η^2 -alkyne pentacoordinated intermediates $[\text{Rh}(\text{PhBP}_3)(\text{HC}\equiv\text{CR})\text{L}]$, which have been observed by low-temperature NMR studies or even isolated, as in the case of $[\text{Rh}(\text{PhBP}_3)(\text{HC}\equiv\text{CCO}_2\text{Me})(\text{PMe}_3)]$.

Other weaker ligands such as acetonitrile also promote the C–H bond cleavage of terminal alkynes, as confirmed by the observation of $[\text{Rh}(\text{PhBP}_3)(\text{H})(\text{C}\equiv\text{CPh})(\text{NCMe})]$ on dissolving $[\text{Rh}(\text{PhBP}_3)(\text{HC}\equiv\text{CPh})]$ in acetonitrile. In this line, DFT-calculations on intermediates **11** and **12** having the alkyne coordinated through the C–H bond (previous to the C–H bond cleavage step) revealed that **12** is stabilized by 9.3 kcal mol⁻¹ upon acetonitrile coordination. These results support the relevant role of pentacoordinated intermediates of the type $[\text{Rh}(\text{PhBP}_3)(\text{HC}\equiv\text{CPh})(\text{L})]$ in which the alkyne undergoes a change of the coordination mode from $\eta^2\text{-C}\equiv\text{C}$ to $\eta^2\text{-C-H}$ behaving as a 2e⁻ donor.

C–H activation for iridium complexes is highly disfavoured even with the basic PMe_3 ligand, and the reaction stops at the pentacoordinate complex $[\text{Ir}(\text{PhBP}_3)(\text{HC}\equiv\text{CPh})(\text{PMe}_3)]$. This divergence in the reactivity of rhodium vs iridium complexes is associated to the strength of the M–alkyne bond, which prevents the slippage of the alkyne to get the C–H coordination mode in iridium complexes.

The hydrido alkynyl rhodium complexes having the labile acetonitrile as coligand are suitable to bind a new molecule of alkyne, which promotes hydride insertion and C–C bond formation to give the *E*-enynes compounds $[\text{Rh}(\text{PhBP}_3)(\text{RC}\equiv\text{C-CH=CHR})]$ (R = Ph; *p*-tol). In these complexes rhodium was found to be again in a pseudo-tetrahedral environment $\eta^2\text{-C}\equiv\text{C}$ bound to the enyne, despite the close C=C bond suitable for coordination.

Catalytic reactions to enynes by using $[\text{Rh}(\text{PhBP}_3)(\text{C}_2\text{H}_4)(\text{NCMe})]\cdot 2\text{MeCN}$ (**2**) as precatalyst proceed under smooth conditions and high regioselectivities to the *E* isomers. The reactions work very well in acetonitrile, which is expected according to the above comments. Remarkably, complex **2** is one the faster precatalyst for alkyne-dimerization reported up to date. For the particular case of $[\text{Rh}(\text{PhBP}_3)(\text{HC}\equiv\text{CCO}_2\text{Me})]$, where C–H bond activation process is slow, cyclotrimerization of methyl propiolate to the arene 1,3,5-C₆H₃(CO₂Me)₂ was observed.

Finally, this report highlights the notable versatility of the 'Rh(PhBP₃)' platform in C–C bond formation either through insertion or cycloaddition reactions for the synthesis of *E*-enynes or arenes, respectively. The *E* selectivity in the synthesis of enynes can be attributed to the steric crowding provided by the $[\text{PhBP}_3]^-$ ligand, while the nature of the alkyne tips the balance towards dimerization vs cycloaddition reactions. We believe that the findings reported here will help the improvement of existing catalytic methods, as well as the development of new catalysts for organic transformations.

Experimental Section

General methods: All operations were carried out under an argon atmosphere using standard Schlenk techniques. Organic solvents were dried by standard procedures and distilled under argon prior to use or obtained oxygen- and water-free from a Solvent Purification System. Complexes $[\{\text{Ir}(\text{coe})_2(\mu\text{-Cl})_2\}_2]$,^[1, 53] $[\{\text{Ir}(\text{C}_2\text{H}_4)_2(\mu\text{-Cl})_2\}_2]$,^[1, 54] $[\text{Rh}(\text{PhBP}_3)(\text{C}_2\text{H}_4)(\text{NCMe})]\cdot 2\text{MeCN}$ (**2**),^[26] and $[\text{Li}(\text{tmen})][\text{PhB}(\text{CH}_2\text{PPh}_2)_3]$ ^[27] were prepared according to the literature methods. Phenylacetylene was distilled under vacuum. Other reagents were commercially available and were used as received. Carbon, hydrogen, and nitrogen analyses were carried out with a Perkin-Elmer 2400 CHNS/O microanalyzer. Mass spectra of complexes were acquired on an Esquire3000 plus (ESI+) spectrometer in acetonitrile. NMR spectra were recorded on Bruker AV 300, AV 400 and AV 500 spectrometers operating at 300.13, 400.13 and 500.13 MHz, respectively, for ¹H. Chemical shifts are reported in ppm and referenced to SiMe₄, using the internal signal of the deuterated solvent (¹H and ¹³C) and external H₃PO₄ (³¹P). IR spectra of solid samples were recorded with a Perkin-Elmer 100 FT-IR spectrometer (4000–400 cm⁻¹) equipped with attenuated total reflectance (ATR).

Synthesis of representative complexes (see the Supporting Information for the compounds not included here):

$[\text{Ir}(\text{PhBP}_3)(\text{C}_2\text{H}_4)(\text{NCMe})]$ (1**).** A Schlenk tube was charged with solid $[\{\text{Ir}(\text{C}_2\text{H}_4)_2(\mu\text{-Cl})_2\}_2]$ (120.0 mg, 0.211 mmol) and solid $[\text{Li}(\text{tmen})][\text{PhB}(\text{CH}_2\text{PPh}_2)_3]$ (338.0 mg, 0.423 mmol). Addition of degassed acetonitrile (3 mL) dissolved the starting materials while a white crystalline solid precipitated almost immediately. After stirring for 30 min, the solid was separated by decantation, washed with a mixture of water/acetonitrile (1:2, 3 x 3 mL) and vacuum-dried. Yield: 407.6 mg (58%). ¹H NMR (300.13 MHz, CD₂Cl₂, 25 °C): δ = 7.92 (br s, 4H, Ph₂^oP^M), 7.63 (br d, ³J(H,H) = 7.1 Hz, 2H, BPh^o), 7.33 (m, 8H, Ph₂^(m+p)P^M + BPh^m), 7.04 (m, 13H, BPh^p + Ph₂^(o+m+p)P^M + Ph₂^pP^A), 6.80 (m, 8H, Ph₂^(o+m)P^A), 1.86 (br d, ³J(H,H) = 6.2 Hz, 4H, C₂H₄ + CH₂P), 1.56 (s, 3H, NCMe), 1.41 (m, 4H, CH₂P), 1.15 (m, 2H, C₂H₄). ³¹P{¹H} NMR (121.5 MHz, CD₂Cl₂, 25 °C): δ = -10.4 (t, 1P, ²J(P,P) = 23 Hz, P^A), -12.5 (d, 2P, ²J(P,P) = 23 Hz, P^M). Selected ¹³C{¹H} NMR (75.5 MHz, CD₂Cl₂, 25 °C) resonances

obtained from ^1H , ^{13}C -hsqc and ^1H , ^{13}C -hmbc spectra: $\delta = 113.9$ (NCMe), 16.6 (C_2H_4), 3.2 (NCMe). MS (ESI⁺): m/z (%): 878 (100) $[(\text{PhBP}_3)\text{Ir}]^+$. Anal. Calcd (%) for $\text{C}_{49}\text{H}_{48}\text{NBP}_3\text{Ir}$ (946.86): C 62.16, H 5.11, N 1.48; found: C 61.98, H 5.17, N 1.55.

[Ir(PhBP₃)(HC≡CPh)] (3). Freshly distilled PhC≡CH (7.6 μL, 0.070 mmol) was added to a solution of $[\text{Ir}(\text{PhBP}_3)(\text{C}_2\text{H}_4)(\text{NCMe})]$ (**1**) (65.8 mg, 0.070 mmol) in toluene (5 mL). An immediate color change of the solution to orange took place. After stirring for 45 min, the volatiles were evaporated to ca. 1 mL under vacuum and the solution was carefully layered with hexane to render orange microcrystals in two days. The solution was decanted and the crystals were washed with hexane and vacuum-dried. Yield: 54.18 mg (79%). ^1H NMR (500.13 MHz, CD_2Cl_2 , 25 °C): $\delta = 11.77$ (q, $^3J(\text{H},\text{P}) = 7.2$ Hz, 1H, HC≡), 7.78 (d, $^3J(\text{H},\text{H}) = 7.2$ Hz, 2H, BPh^o), 7.59 (m, 2H, ≡CPh^o), 7.37 (m, 5H, BPh^o, ≡CPh^m), 7.33 (t, $^3J(\text{H},\text{H}) = ^3J(\text{H},\text{P}) = 8.8$ Hz, 12H, Ph₂^oP), 7.03 (tt, $^3J(\text{H},\text{H}) = 7.3$, $^4J(\text{H},\text{H}) = 1.2$ Hz, 1H, Ph₂^p), 6.92 (t, $^3J(\text{H},\text{H}) = 7.3$ Hz, 12H, Ph₂^mP), 1.65 (d, $^2J(\text{H},\text{P}) = 11.2$ Hz, 6H, CH₂P). $^{31}\text{P}\{^1\text{H}\}$ NMR (202.5 MHz, CD_2Cl_2 , 25 °C): $\delta = 14.6$ (s). Selected $^{13}\text{C}\{^1\text{H}\}$ NMR (125.8 MHz, CD_2Cl_2 , 25 °C) resonances obtained from ^1H , ^{13}C -hsqc and ^1H , ^{13}C -hmbc spectra: $\delta = 179.8$ (≡CPh), 166.3 (HC≡), 138.7 (≡CPh^{iso}), 131.2 (≡CPh^o), 128.3 (≡CPh^m), 127.8 (≡CPh^p). IR (ATR): $\nu(\text{C}\equiv\text{C})/\text{cm}^{-1}$: 1664. MS(ESI⁺): m/z (%): 979.1 (15) $[\text{M}-\text{H}]$. Anal. Calcd (%) for $\text{C}_{53}\text{H}_{47}\text{BP}_3\text{Ir}$ (979.89): C 64.96, H 4.83; found: C 66.50, H 4.98.

[Rh(PhBP₃)(HC≡CPh)] (6). Freshly distilled PhC≡CH (7.7 μL, 0.07 mmol) was added to a solution of $[\text{Rh}(\text{PhBP}_3)(\text{C}_2\text{H}_4)(\text{NCMe})]\cdot 2\text{MeCN}$ (65.8 mg, 0.07 mmol) in toluene (5 mL). An immediate color change of the solution from orange to dark-red took place. After stirring for 15 min, the volatiles were evaporated under vacuum to ca. 1 mL and the solution was carefully layered with hexane to render dark-red microcrystals in two days. The solution was decanted, and the crystals were washed with hexane and vacuum-dried. Yield: 47.4 mg (76%). ^1H NMR (400 MHz, C_6D_6 , 25 °C): $\delta = 10.04$ (qd, $^3J(\text{H},\text{P}) = 10.5$ Hz, $^2J(\text{H},\text{Rh}) = 1.7$ Hz, 1H, HC≡), 8.22 (d, $^3J(\text{H},\text{H}) = 7.3$ Hz, 2H, BPh^o), 7.75 (t, $^3J(\text{H},\text{H}) = 7.5$ Hz, 2H, BPh^m), 7.66 (dd, $J(\text{H},\text{H}) = 8.5$, 1.6 Hz, 2H, ≡CPh^o), 7.49 (tt, $J(\text{H},\text{H}) = 7.3$, 1.4 Hz, 1H, BPh^p), 7.38 (t, $^3J(\text{H},\text{H}) = ^3J(\text{H},\text{P}) = 8.5$ Hz, 12H, Ph₂^oP), 7.19 (tt, $J(\text{H},\text{H}) = 7.5$, 1.2 Hz, 2H, ≡CPh^m), 7.11 (tt, $J(\text{H},\text{H}) = 7.2$, 1.3, 1H, ≡CPh^p), 6.74 (td, $J(\text{H},\text{H}) = 7.1$, 1.2 Hz, 6H, Ph₂^pP), 6.68 (td, $J(\text{H},\text{H}) = 7.9$, 1.3 Hz, 12H, Ph₂^mP), 1.88 (d, $^3J(\text{H},\text{P}) = 10.9$ Hz, 6H, CH₂P). $^{31}\text{P}\{^1\text{H}\}$ NMR (162 MHz, C_6D_6 , 25 °C): $\delta = 47.7$ (d, $J_{\text{P,Rh}} = 110$ Hz). Selected ^{13}C NMR resonances obtained from ^1H , ^{13}C -hsqc and ^1H , ^{13}C -hmbc spectra: $\delta = 164.9$ (≡CPh), 151.8 (HC≡), 138.1 (≡CPh^{iso}), 130.2 (≡CPh^o), 128.2 (≡CPh^m), 127.5 (≡CPh^p). IR (ATR): $\nu(\text{C}\equiv\text{C})/\text{cm}^{-1}$: 1661 (w). MS (ESI⁺): m/z (%): 890.6 (100) $[\text{M}]^+$. Anal. Calcd (%) for $\text{C}_{53}\text{H}_{47}\text{BP}_3\text{Rh}$ (890.58): C 71.48, H 5.32; found: C 71.74, H 5.31.

[Rh(PhBP₃)(H₂C=CHPh)(NCMe)] (13) was prepared by addition of styrene in excess (84.1 μL, 0.734 mmol) to a yellow solution of $[\text{Rh}(\text{PhBP}_3)(\text{C}_2\text{H}_4)(\text{NCMe})]\cdot 2\text{MeCN}$ (115.0 mg, 0.122 mmol) in toluene (2 mL). An immediate color change to dark orange took place. After 4 vacuum/argon cycles in order to displace the equilibrium to complex **13**, and 40 min. at room temperature, hexane (8 mL) was added producing the precipitation of an orange solid. The solid was washed with cold hexane (4 x 2 mL), decanted and vacuum dried. Yield: 89.4 (82%). ^1H NMR (300.13 MHz, C_6D_6 , 25 °C): $\delta = 8.49$ -6.51 (40H, Ph), 4.43 (q, $^3J(\text{H},\text{H}) = 8.3$ Hz, 1H, CH₂=CHPh), 3.12 (m, $^3J(\text{H},\text{H}) = 10.9$ Hz, 1H, CH₂=CHPh), 2.45 (m, 1H, CH₂P^C), 2.25 (m, 1H, CH₂P^A), 2.09 (m, 1H, CH₂P^C), 1.92 (m, 1H, CH₂P^B), 1.82 (m, 1H, CH₂P^B), 1.76 (m, 1H, CH₂=CHPh), 0.46 (br s, 3H, NCMe). $^{31}\text{P}\{^1\text{H}\}$ RMN (121.5 MHz, C_6D_6 , 25°): $\delta = 43.9$ (dt, $J(\text{P},\text{Rh}) = 122$ Hz, $^2J(\text{P},\text{P}) = 33$ Hz, 1P, P^A), 18.8 (ddd, $J(\text{P},\text{Rh}) = 83$ Hz, $^2J(\text{P},\text{P}) = 51$ Hz, $^2J(\text{P},\text{P}) = 33$ Hz, 1P, P^C), 5.90 (ddd, $J(\text{P},\text{Rh}) = 106$ Hz, $^2J(\text{P},\text{P}) = 50$ Hz, $^2J(\text{P},\text{P}) = 33$ Hz, 1P, P^B).

[Ir(PhBP₃)(HC≡CPh)(PMe₃)] (14). Trimethylphosphane (1M in toluene, 86.7 μL, 0.087 mmol) was added to a solution of $[\text{Ir}(\text{PhBP}_3)(\text{HC}\equiv\text{CPh})]$ (**3**) (85.0 mg, 0.087 mmol) in toluene (5 mL) producing an immediate color change from red to yellow. The solution was evaporated to ca. 0.5 mL and precipitated with hexane (6 mL) yielding a beige solid. The solution was decanted and the solid was washed with hexane (2 x 2 mL) and vacuum-dried. Yield: 77.8 mg (85%). $^1\text{H}\{^{31}\text{P}\}$ NMR (400.13 MHz, C_6D_6 , 25 °C): $\delta = 8.19$ (d, $^3J(\text{H},\text{H}) = 7.6$ Hz, 2H, BPh^o), 8.13 (d, $^3J(\text{H},\text{H}) = 7.4$ Hz, 2H, Ph₂^oP^C), 7.82 (d, $^3J(\text{H},\text{H}) = 6.8$ Hz, 2H, Ph^o), 7.66 (t, $^3J(\text{H},\text{H}) = 7.4$ Hz, 2H, BPh^m), 7.63 (d, $^3J(\text{H},\text{H}) = 7.0$ Hz, 2H, Ph₂^oP^C), 7.44 (m, 9H, BPh^p + Ph₂^{o(1+2)}P^A + Ph₂^{o(1+2)}P^B), 7.24 (t, $^3J(\text{H},\text{H}) = 7.6$ Hz, 2H, Ph^m), 7.10 (m, 1H, Ph^o), 7.02 (t, $^3J(\text{H},\text{H}) = 7.1$ Hz, 1H, Ph₂^oP^C), 6.79 (m, 13H, Ph₂^{(m+p)1}P^B + Ph₂^{(m+p)2}P^B + Ph₂^{o(1+2)}P^A + Ph₂^{m(1+2)}P^C + Ph₂^{p2}P^C), 6.61 (t, $^3J(\text{H},\text{H}) = 7.5$ Hz, 2H, Ph₂^{m1}P^A), 6.59 (t, $^3J(\text{H},\text{H}) = 8.0$ Hz, 2H, Ph₂^{m2}P^A), 6.13 (s, 1H, HC≡), 2.45 (br s, 2H, CH₂P^C), 2.36 (d, $^2J(\text{H},\text{H}) = 15.6$ Hz, 1H, CH₂P^B), 2.10 (d, $^2J(\text{H},\text{H}) = 15.6$ Hz, 1H, CH₂P^B), 1.89 (d, $^2J(\text{H},\text{H}) = 14.7$ Hz, 1H, CH₂P^A), 1.47 (d, $^2J(\text{H},\text{H}) = 14.7$ Hz, 1H, CH₂P^A), 0.25 (s, 9H, (PMe₃)). $^{31}\text{P}\{^1\text{H}\}$ NMR (162.0 MHz, C_6D_6 , 25 °C): $\delta = -7.7$ (td, $^2J(\text{P},\text{P}) = 27$ Hz, $^2J(\text{P},\text{P}) = 19$ Hz, P^C), -17.8 (td, $^2J(\text{P},\text{P}) = 26$ Hz, $^2J(\text{P},\text{P}) = 19$ Hz, P^B), -39.6 (dt, $^2J(\text{P},\text{P}) = 424$ Hz, $^2J(\text{P},\text{P}) = 26$ Hz, P^A), -47.6 (dt, $^2J(\text{P},\text{P}) = 424$ Hz, $^2J(\text{P},\text{P}) = 19$ Hz, P^M). Selected $^{13}\text{C}\{^1\text{H}\}$ NMR (100.6 MHz, C_6D_6 , 25 °C) resonances obtained from ^1H , ^{13}C -hsqc and ^1H , ^{13}C -hmbc spectra: $\delta = 131.6$ (C^{iso}), 131.1 (Ph^o), 127.6 (Ph^m), 125.6 (Ph^p), 89.0 (≡CPh), 83.1 (HC≡), 14.7 (PMe₃). IR (ATR): $\nu(\text{C}\equiv\text{C})/\text{cm}^{-1}$: 1669 (w). Anal. Calcd. (%) for $\text{C}_{56}\text{H}_{56}\text{BP}_4\text{Ir}$ (1055.97): C 63.70, H 5.35; found: C 63.86, H 5.30.

[Rh(PhBP₃)(HC≡CCO₂Me)(PMe₃)] (18). Trimethylphosphane (1M in toluene, 126.1 μL, 0.126 mmol) was added to a solution of $[\text{Rh}(\text{PhBP}_3)(\text{HC}\equiv\text{CCO}_2\text{Me})]$ (**11**) (110.0 mg, 0.126 mmol) in toluene (5 mL), producing an immediate color change from red to orange. The solution was evaporated to ca. 0.5 mL and the product was precipitated with hexane (6 mL) as an orange solid. The solution was decanted and the solid was washed with hexane (2 x 2 mL) and vacuum-dried. Yield: 89.7 mg (75%). $^1\text{H}\{^{31}\text{P}\}$ NMR (400.13 MHz, C_6D_6 , 25 °C): $\delta = 8.45$ (br s, 2H, Ph₂^oP^B), 8.21 (d, $^3J(\text{H},\text{H}) = 6.3$ Hz, 2H, BPh^o), 8.03 (d, $^3J(\text{H},\text{H}) = 6.6$ Hz, 2H, Ph₂^oP^C), 7.66 (t, $^3J(\text{H},\text{H}) = 7.2$ Hz, 2H, BPh^m), 7.62 (d, $^3J(\text{H},\text{H}) = 7.0$ Hz, 2H, Ph₂^oP^B), 7.41 (d, $^3J(\text{H},\text{H}) = 7.6$ Hz, 2H, Ph₂^oP^A), 7.38 (m, 1H, BPh^p), 7.33 (d, $^3J(\text{H},\text{H}) = 6.3$ Hz, 2H, Ph₂^oP^C), 7.24 (t, $^3J(\text{H},\text{H}) = 7.2$ Hz, 2H, Ph₂^mP^B), 7.12 (t, $^3J(\text{H},\text{H}) = 7.3$ Hz, 1H, Ph₂^oP^A), 7.04 (d, $^3J(\text{H},\text{H}) = 7.03$, 2H, Ph₂^oP^A), 6.98 (m, 3H, Ph₂^mP^C + Ph₂^oP^B), 6.80 (m, 4H, HC≡ + Ph₂^{(m+p)2}P^B), 6.74 (m, 7H, Ph₂^{(m+p)2}P^A + Ph₂^{(m+p)2}P^C + Ph₂^oP^C), 6.62 (t, $^3J(\text{H},\text{H}) = 7.4$ Hz, 2H, Ph₂^{m1}P^A), 3.69 (s, 3H, CO₂Me), 2.25 (m, 3H, CH₂P^B + CH₂P^C), 1.88 (br d, $^2J(\text{H},\text{H}) = 14.6$ Hz, 1H, CH₂P^C), 1.68 (br s, 2H, CH₂P^A), 0.34 (s, 9H, PMe₃). $^{31}\text{P}\{^1\text{H}\}$ NMR (162.0 MHz, C_6D_6 , 25 °C): $\delta = 22.0$ (ddd, $J(\text{P},\text{Rh}) = 117$ Hz, $^2J(\text{P},\text{P}) = 37$ Hz, $^2J(\text{P},\text{P}) = 27.0$ Hz, P^C), 18.0 (ddd, $J(\text{P},\text{Rh}) = 107$ Hz, $^2J(\text{P},\text{P}) = 37$ Hz, $^2J(\text{P},\text{P}) = 31$ Hz, P^B), 12.8 (dt, $^2J(\text{P},\text{P}) = 454$ Hz, $J(\text{P},\text{Rh}) = 84$ Hz, $^2J(\text{P},\text{P}) = 37$ Hz, P^A), -11.2 (dddd, $^2J(\text{P},\text{P}) = 454$ Hz, $J(\text{P},\text{Rh}) = 94$ Hz, $^2J(\text{P},\text{P}) = 31$ Hz, $^2J(\text{P},\text{P}) = 27$ Hz, P^M). Selected $^{13}\text{C}\{^1\text{H}\}$ NMR (100.6 MHz, C_6D_6 , 25 °C) resonances obtained from ^1H , ^{13}C -hsqc and ^1H , ^{13}C -hmbc: $\delta = 166.3$ (CO₂Me), 111.3 (HC≡), 87.9 (≡CCO₂Me), 51.2 (CO₂Me), 15.7 (PMe₃). IR (ATR): $\nu(\text{CO}_2\text{CH}_3)/\text{cm}^{-1}$: 1708, $\nu(\text{C}\equiv\text{C})/\text{cm}^{-1}$: 1664. Anal. Calcd. (%) for $\text{C}_{52}\text{H}_{54}\text{BP}_4\text{O}_2\text{Rh}$ (948.60): C 65.84, H 5.74; found: C 66.04, H 5.30.

[Rh(PhBP₃)(C≡CCO₂Me)(H)(PMe₃)] (19). was prepared 'in situ' by complete conversion of a solution of $[\text{Rh}(\text{PhBP}_3)(\text{HC}\equiv\text{CCO}_2\text{Me})(\text{PMe}_3)]$ (**18**) (25.0 mg, 0.029 mmol) into **19** after 7 days at room temperature. Single microcrystals for X-ray diffraction studies were grown in C_6D_6 . $^1\text{H}\{^{31}\text{P}\}$ NMR (300.13 MHz, C_6D_6 , 25 °C): $\delta = 8.19$ (d, $^3J(\text{H},\text{H}) = 6.7$ Hz, 2H, BPh^o), 8.13 (m, 2H, Ph₂^oP^A), 8.01 (m, 6H, Ph₂^oP^B + Ph₂^oP^C + Ph₂^oP^A), 7.68 (t, $^3J(\text{H},\text{H}) = 7.5$ Hz, 2H, BPh^m), 7.48 (m, 2H, Ph₂^oP^B), 7.42 (t, $^3J(\text{H},\text{H}) = 7.3$ Hz, 1H, BPh^p), 7.20 (m, 2H, Ph₂^oP^C), 6.98 (m, 6H, Ph₂^{(m+p)1}P^A + Ph₂^{(m+p)1}P^B), 6.86 (m, 3H, Ph₂^{(m+p)2}P^B), 6.71 (m, 9H,

$\text{Ph}_2^{(m+p)2}\text{P}^{\text{C}} + \text{Ph}_2^{(m+p)1}\text{P}^{\text{C}} + \text{Ph}_2^{(m+p)2}\text{P}^{\text{A}}$, 3.58 (s, 3H, CO_2CH_3), 2.30 (m, 2H, $\text{CH}_2\text{P}^{\text{B+C}}$), 2.13 (d, $^3\text{J}(\text{H,H}) = 15.5$ Hz, 1H, $\text{CH}_2\text{P}^{\text{B}}$), 1.97 (d, $^3\text{J}(\text{H,H}) = 14.4$ Hz, 1H, $\text{CH}_2\text{P}^{\text{B}}$), 1.91 (d, $^2\text{J}(\text{H,H}) = 14.6$ Hz, 1H, $\text{CH}_2\text{P}^{\text{A}}$), 1.32 (d, $^2\text{J}(\text{H,H}) = 14.5$ Hz, 1H, $\text{CH}_2\text{P}^{\text{A}}$), 0.65 (s, 9H, PMe_3), -8.74 (d, $\text{J}(\text{H,Rh}) = 14.5$ Hz, 1H, Rh-H). $^{31}\text{P}\{^1\text{H}\}$ NMR (121.5 MHz, C_6D_6 , 25 °C): $\delta = 27.4$ (ddt, $\text{J}(\text{P,Rh}) = 90$ Hz, $^2\text{J}(\text{P,P}) = 36$ Hz, $^2\text{J}(\text{P,P}) = 23$ Hz, P^{C}), 19.7 (ddt, $^2\text{J}(\text{P,P}) = 341$ Hz, $\text{J}(\text{P,Rh}) = 82$ Hz, $^2\text{J}(\text{P,P}) = 35$ Hz, P^{A}), 5.4 (ddt, $\text{J}(\text{P,Rh}) = 72$ Hz, $^2\text{J}(\text{P,P}) = 35$ Hz, $^2\text{J}(\text{P,P}) = 23$ Hz, P^{B}), -11.6 (ddt, $^2\text{J}(\text{P,P}) = 341$ Hz, $\text{J}(\text{P,Rh}) = 87$ Hz, $^2\text{J}(\text{P,P}) = 23$ Hz, P^{M}).

[Rh(PhBP₃)(PhC≡C-CH=CHPh)] (20). [Rh(PhBP₃)(C₂H₄)(NCMe)] (22.7 mg, 0.03 mmol) was dissolved in C_6D_6 (0.5 mL) and freshly distilled $\text{PhC}\equiv\text{CH}$ (5.8 μL , 0.05 mmol) was added. An immediate color change of the solution from orange to dark-red was observed. The course of the reaction was monitored by ^1H NMR spectroscopy and the complete conversion was reached after ca. 8h at rt. The solution was then evaporated to ca. 0.1 mL and layered with hexane to render dark-red microcrystals in two days. The crystals were decanted, washed with hexane and vacuum-dried. Yield: 16.3 mg (62%). $^1\text{H}\{^{31}\text{P}\}$ NMR (300 MHz, C_6D_6 , 25 °C) (integrals were taken from the usual ^1H NMR spectrum): $\delta = 8.21$ (d, $^3\text{J}(\text{H,H}) = 8.8$ Hz, 2H, BPh^{O}), 8.09 (dd, $^3\text{J}(\text{H,H}) = 15.7$ Hz, $^4\text{J}(\text{H,Rh}) = 1.8$ Hz, 1H, $\text{Ph}^{\text{B}}\text{CH}=\text{CH}-\text{C}\equiv\text{C}-\text{Ph}^{\text{A}}$), 7.74 (t, $^3\text{J}(\text{H,H}) = 7.3$ Hz, 2H, BPh^{M}), 7.71 (dd, $^3\text{J}(\text{H,H}) = 6.9$, 1.3 Hz, 2H, $\text{Ph}^{\text{A}^{\text{O}}}$), 7.48 (tt, $^3\text{J}(\text{H,H}) = 7.2$, 1.4 Hz, 1H, BPh^{P}), 7.40 (dd, $^3\text{J}(\text{H,H}) = 6.8$, 1.7 Hz, 12H, $\text{Ph}_2^{\text{O}^{\text{P}}}$), 7.30 (dd, $^3\text{J}(\text{H,H}) = 8.4$, 1.4 Hz, 2H, $\text{Ph}^{\text{B}^{\text{O}}}$), 7.25 (tt, $^3\text{J}(\text{H,H}) = 7.7$, 1.4 Hz, 2H, $\text{Ph}^{\text{A}^{\text{M}}}$), 7.14 (t, $^3\text{J}(\text{H,H}) = 7.4$ Hz, 1H, $\text{Ph}^{\text{A}^{\text{O}}}$), 7.09 (t, $^3\text{J}(\text{H,H}) = 7.1$, 2H, $\text{Ph}^{\text{B}^{\text{M}}}$), 7.07 (d, $^3\text{J}(\text{H,H}) = 15.7$ Hz, 1H, $\text{Ph}^{\text{B}}\text{CH}=\text{CH}-\text{C}\equiv\text{C}-\text{Ph}^{\text{A}}$), 7.05 (t, $^3\text{J}(\text{H,H}) = 7.0$ Hz, 1H, $\text{Ph}^{\text{B}^{\text{O}}}$), 6.76 (tt, $^3\text{J}(\text{H,H}) = 7.4$, 1.4 Hz, 6H, $\text{Ph}_2^{\text{O}^{\text{P}}}$), 6.69 (tt, $^3\text{J}(\text{H,H}) = 6.9$, 1.7 Hz, 12H, $\text{Ph}_2^{\text{M}^{\text{P}}}$), 1.91 (br s, 6H, CH_2P). $^{31}\text{P}\{^1\text{H}\}$ NMR (121 MHz, C_6D_6 , 25 °C): $\delta = 45.8$ (d, $\text{J}(\text{P,Rh}) = 110$ Hz). Selected ^{13}C NMR resonances obtained from hsqc and hmbc spectra: $\delta = 167.4$ ($\text{Ph}^{\text{B}}\text{CH}=\text{CH}-\text{C}\equiv\text{C}-\text{Ph}^{\text{A}}$), 161.8 ($\text{Ph}^{\text{B}}\text{CH}=\text{CH}-\text{C}\equiv\text{C}-\text{Ph}^{\text{A}}$), 136.3 ($\text{Ph}^{\text{B}}\text{CH}=\text{CH}-\text{C}\equiv\text{C}-\text{Ph}^{\text{A}}$), 128.8 ($\text{Ph}^{\text{A}^{\text{M}}}$), 128.7 ($\text{Ph}^{\text{A}^{\text{O}}}$), 128.16 ($\text{Ph}^{\text{B}^{\text{M}}}$), 128.15 ($\text{Ph}^{\text{B}^{\text{O}}}$), 127.2 ($\text{Ph}^{\text{B}^{\text{O}}}$), 127.1 ($\text{Ph}^{\text{A}^{\text{O}}}$), 123.6 ($\text{Ph}^{\text{B}}\text{CH}=\text{CH}-\text{C}\equiv\text{C}-\text{Ph}^{\text{A}}$). IR (ATR): $\nu(\text{C}\equiv\text{C})/\text{cm}^{-1}$: 1665. MS (ESI⁺): m/z (%): 994.2 (6) [$\text{M}+2\text{H}$]⁺, 789.2 (62) [$\text{M}-\text{eneyne}+\text{H}$]⁺. Anal. Calcd (%) for $\text{C}_{61}\text{H}_{53}\text{BP}_3\text{Rh}$ (992.71): C 73.80, H 5.38; found: C 73.61, H 5.30.

Catalytic essays.

Catalytic alkyne dimerization reactions: A NMR tube containing a solution of the catalyst with loads of 5%, 1% or 0.1% mol% in either [D_8]-toluene or CD_3CN (0.5 mL) was treated with the alkyne (1.00 mmol) and warmed to the indicated temperature. The reaction course was monitored by ^1H NMR spectroscopy, and the conversion was determined by integration of the corresponding resonances of the alkyne and the enynes. Catalytic cyclotrimerization of methyl propiolate: A NMR tube containing a solution of catalyst (0.01 mmol) in either [D_8]-toluene or CD_3CN (0.5 mL) was treated with methyl propiolate (0.20 mmol) and warmed to the indicated temperature. The reaction course was monitored by ^1H NMR spectroscopy, and the conversion was determined by integration of the corresponding resonances of the alkyne and tri(carboxymethyl)benzene.

DFT geometry optimizations. The DFT geometry optimizations and calculations were carried out with the Gaussian 09 program package,^[55] using the B3LYP-D3 hybrid functional.^[56] Geometry optimizations were performed in the gas phase with the LanL2TZ(f) effective core potential basis set for the metal atoms, and the 6-311G(d,p) basis set for the remaining ones.

X-ray diffraction studies on complexes 3·C₇H₈ and 19·2C₆H₆. Intensity measurements were collected with a Smart Apex diffractometer, with graphite-monochromated $\text{MoK}\alpha$ radiation. A semi-empirical absorption correction was applied to each data set, with the multi-scan^[57] methods.

Selected crystallographic data can be found in the Supporting Information. The structures were solved by direct methods and refined by full-matrix least-squares, with the program SHELXL-2016^[58] in the WINGX^[59] package. Hydrogen atoms were geometrically calculated and refined by the riding mode, including the isotropic displacement parameters. All non-hydrogen atoms were refined with anisotropic displacement parameters except the ones of the minor fraction (occupancy 0.148(7)) of a disorder modelled in (19·2C₆H₆); this disorder ligand was refined with geometrical constraints. CCDC 1855476 (3·C₇H₈) and 1855269 (19·2C₆H₆) contain the supplementary crystallographic data for this paper. These data can be obtained free of charge from The Cambridge Crystallographic Data Centre via www.ccdc.cam.ac.uk/data_request/cif.

Selected crystallographic data for [[r(PhBP₃)(HC≡CPh)]·C₇H₈ (3·C₇H₈). Crystal data for 3·C₇H₈: $\text{C}_{60}\text{H}_{55}\text{BrP}_3$, $M_r = 1071.96$, triclinic, space group P-1, $a = 10.9698(12)$, $b = 13.1865(14)$, $c = 16.7637(18)$ Å, $\alpha = 87.958(2)$, $\beta = 80.720(2)$, $\gamma = 87.178(2)^\circ$, $V = 2389.3(4)$ Å³, $Z = 2$, $\rho_{\text{calcd}} = 1.490$ g cm⁻³, $F(000) = 1084$, $T = 100(2)$ K, $\text{MoK}\alpha$ radiation ($\lambda = 0.71073$ Å, $\mu = 2.935$ mm⁻¹). Data were collected with a dark orange irregular block (0.46 × 0.08 × 0.01 mm). Of 13086 measured reflections (2θ 3.1–52.0°), 9239 were unique ($R_{\text{int}} = 0.0430$). Final agreement factors were $R_1 = 0.0575$ (7610 observed reflections) and $wR_2 = 0.1129$. Data/restraints/parameters 9239/0/586; GOF = 1.081. Largest peak and hole in the final difference map 1.456 and -2.001 e Å⁻³.

Selected crystallographic data for [Rh(PhBP₃)(C≡CCO₂Me)(H)(PMe₃)·2C₆H₆ (19·2C₆H₆). Crystal data for 19·2C₆H₆: $\text{C}_{64}\text{H}_{66}\text{BO}_2\text{P}_4\text{Rh}$, $M_r = 1104.76$, monoclinic, space group P2₁/c, $a = 18.1205(13)$, $b = 10.1578(7)$, $c = 30.375(2)$ Å, $\beta = 106.3300(10)$, $V = 5365.4(7)$ Å³, $Z = 4$, $\rho_{\text{calcd}} = 1.368$ g cm⁻³, $F(000) = 2304$, $T = 100(2)$ K, $\text{MoK}\alpha$ radiation ($\lambda = 0.71073$ Å, $\mu = 0.483$ mm⁻¹). Data were collected with a pale yellow irregular block (0.35 × 0.12 × 0.08 mm). Of 60721 measured reflections (2θ 3.1–54.0°), 11694 were unique ($R_{\text{int}} = 0.0415$). Final agreement factors were $R_1 = 0.0578$ (10460 observed reflections) and $wR_2 = 0.1301$. Data/restraints/parameters 11694/37/673; GOF = 1.100. Largest peak and hole in the final difference map 1.433 and -0.859 e Å⁻³.

Acknowledgements

The generous financial support from MINECO/FEDER (Projects CTQ2014-53033-P and CTQ2017-83421-P, C.T.), and Gobierno de Aragón/FEDER (GA/FEDER, Inorganic Molecular Architecture Group E08_17R; C.T.) is gratefully acknowledged. The Centro de Supercomputación de Galicia (CESGA) is also gratefully acknowledged for generous allocation.

Keywords: rhodium • iridium • pseudotetrahedral • C–C coupling • enynes

- [1] a) D. Roy, Yasuhiro Uozumi, *Adv. Synth. Catal.* **2018**, *360*, 602–625; b) M. Bakherad, *Appl. Organometal. Chem.* **2013**, *27*, 125–140; c) R. Chinchilla, C. Nájera, *Chem. Soc. Rev.* **2011**, *40*, 5084–5121; d) G. C. Fortman, S. P. Nolan, *Chem. Soc. Rev.* **2011**, *40*, 5151–5169.
- [2] a) L. D. Caspers, B. J. Nachtsheim, *Chem. Asian J.* **2018**, *13*, 1231–1247; b) X. Jie, Y. Shang, P. Hu, W. Su, *Angew. Chem.* **2013**, *125*, 3718–3721; *Angew. Chem. Int. Ed.* **2013**, *52*, 3630–3633; c) W. Wu, H. Jiang, *Acc. Chem. Res.* **2012**, *45*, 1736–1748; d) S. H. Cho, J. Y. Kim, J. Kwak, S. Chang, *Chem. Soc. Rev.* **2011**, *40*, 5068–5083.

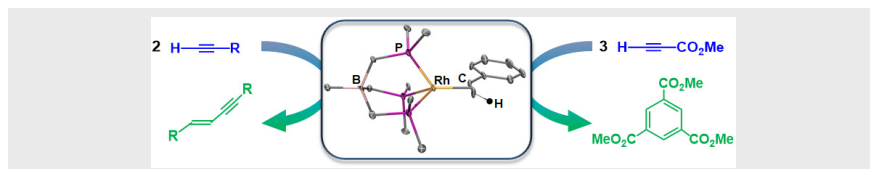
- [3] a) J. Barwick-Silk, S. Hardy, M. C. Willis, A. S. Weller, *J. Am. Chem. Soc.* **2018**, *140*, 7347–7357; b) T. J. Coxon, M. Fernández, J. Barwick-Silk, A. I. McKay, L. E. Britton, A. S. Weller, M. C. Willis, *J. Am. Chem. Soc.* **2017**, *139*, 10142–10149; c) M. Fernández, M. Castaing, Michael C. Willis, *Chem. Sci.* **2017**, *8*, 536–540; d) A. Ghosh, K. F. Johnson, K. L. Vickerman, J. A. Walker, L. M. Stanley, *Org. Chem. Front.* **2016**, *3*, 639–644; e) M. C. Willis, *Chem. Rev.* **2010**, *110*, 725–748.
- [4] a) D. Xu, Q. Sun, Z. Quan, X. Wang, W. Sun, *Asian J. Org. Chem.* **2018**, *7*, 155–159; b) Q. Liang, K. M. Osten, D. Song, *Angew. Chem.* **2017**, *129*, 6414–6417; *Angew. Chem. Int. Ed.* **2017**, *56*, 6317–6320; c) O. Rivada-Wheelaghan, S. Chakraborty, L. J. W. Shimon, Y. Ben-David, D. Milstein, *Angew. Chem.* **2016**, *128*, 7056–7059; *Angew. Chem. Int. Ed.* **2016**, *55*, 6942–6945; d) M. G. Lauer, B. R. Headford, O. M. Gobble, M. B. Weyhaupt, D. L. Gerlach, M. Zeller, K. H. Shaughnessy, *ACS Catal.* **2016**, *6*, 5834–5842; e) Y. Zhou, Y. Zhang, J. Wang, *Org. Biomol. Chem.* **2016**, *14*, 6638–6650; f) J. Alós, T. Bolaño, M. A. Esteruelas, M. Oliván, E. Oñate, M. Valencia, *Inorg. Chem.* **2014**, *53*, 1195–1209; g) H.-D. Xu, R.-W. Zhang, X. Li, S. Huang, W. Tang, W.-H. Hu, *Org. Lett.* **2013**, *15*, 840–843; h) M. Nishiura, Z. Hou, T. Katagiri, H. Tsurugi, T. Satoh, M. Miura, *Chem. Commun.* **2008**, 3405–3407; i) *J. Mol. Catal. A: Chem.* **2004**, *213*, 101–106.
- [5] a) G. Jiang, W. Hu, J. Li, C. Zhu, W. Wu, H. Jiang, *Chem. Commun.* **2018**, *54*, 1746–1749; b) L. D. Caspers, P. Finkbeiner, B. J. Nachtsheim, *Chem. Eur. J.* **2017**, *23*, 2748–2752; c) D. Das, A. X. Sun, D. Seidel, *Angew. Chem.* **2013**, *125*, 3853–3857; *Angew. Chem. Int. Ed.* **2013**, *52*, 3765–3769.
- [6] A. Fürstner, *Angew. Chem.* **2013**, *125*, 2860–2887; *Angew. Chem. Int. Ed.* **2013**, *52*, 2794–2819.
- [7] a) K. C. K. Swamy, A. S. Reddy, K. Sandeep, A. Kalyani, *Tetrahedron Lett.* **2018**, *59*, 419–429; b) C. Oger, L. Balas, T. Durand, J.-M. Galano, *Chem. Rev.* **2013**, *113*, 1313–1350.
- [8] a) M. C. Lipke, A. L. Liberman-Martin, T. D. Tilley *Angew. Chem.* **2017**, *129*, 2298–2335; *Angew. Chem. Int. Ed.* **2017**, *56*, 2260–2294; b) S. C. Bart, E. Lobkovsky, P. J. Chirik, *J. Am. Chem. Soc.* **2004**, *126*, 13794–13807.
- [9] a) M. T. Pirnot, Y. Wang, S. L. Buchwald *Angew. Chem.* **2016**, *128*, 48–57; *Angew. Chem. Int. Ed.* **2016**, *55*, 48–57; b) A. Kumar, P. Ghosh, *Eur. J. Inorg. Chem.* **2012**, 3955–3969.
- [10] a) C. Chen, X. Chen, X. Zhang, S. Wang, W. Rao, P. W. H. Chan, *Adv. Synth. Catal.* **2017**, *359*, 4359–4368; b) A. Marinetti, H. Jullien, A. Voituriez, *Chem. Soc. Rev.* **2012**, *41*, 4884–4908; c) N. D. Paul, S. Mandal, M. Otte, X. Cui, X. P. Zhang, B. de Bruin, *J. Am. Chem. Soc.* **2014**, *136*, 1090–1096; d) X. Cui, X. Xu, L. Wojtas, M. M. Kim, X. P. Zhang, *J. Am. Chem. Soc.* **2012**, *134*, 19981–19984.
- [11] a) R. J. Batrice, J. McKinven, P. L. Arnold, M. S. Eisen, *Organometallics* **2015**, *34*, 4039–4050; b) X.-F. Wu, H. Neumann, M. Beller, *ChemSusChem* **2013**, *6*, 229–241; c) V. A. Peshkov, O. P. Pereshivko, E. V. Van der Eycken, *Chem. Soc. Rev.* **2012**, *41*, 3790–3807; d) N. Weding, M. Hapke, *Chem. Soc. Rev.* **2011**, *40*, 4525–4538; e) P. R. Chopadea, J. Louie, *Adv. Synth. Catal.* **2006**, *348*, 2307–2327.
- [12] a) H. Nuss, N. Claiser, S. Pilet, N. Lugan, E. Despagne-Ayoub, M. Etienne, C. Lecomte, *Dalton Trans.* **2012**, *41*, 6598–6601; b) J. J. Carbo, P. Crochet, M. A. Esteruelas, Y. Jean, A. Lledós, A. M. López, E. Oñate, *Organometallics* **2002**, *21*, 305–314; c) J. L. Templeton, *Adv. Organomet. Chem.* **1989**, *29*, 1–100; d) B. C. Ward, J. L. Templeton, *J. Am. Chem. Soc.* **1980**, *102*, 1532–1538.
- [13] a) C. Bianchini, K. G. Caulton, G. Chardon, M.-L. Doublet, O. Eisenstein, S. A. Jackson, T. J. Johnson, A. Meli, M. Peruzzini, W. E. Streib, A. Vacca, F. Vizza, *Organometallics* **1994**, *13*, 2010–2023; b) C. Bianchini, P. Barbaro, A. Meli, M. Peruzzini, A. Vacca, F. Vizza, *Organometallics* **1993**, *12*, 2505–2514; c) P. Barbaro, C. Bianchini, A. Meli, M. Peruzzini, A. Vacca, F. Vizza, *Organometallics* **1991**, *10*, 2227–2238; d) C. Bianchini, A. Meli, M. Peruzzini, A. Vacca, F. Vizza, *Organometallics* **1991**, *10*, 645–651; e) C. Bianchini, A. Meli, M. Peruzzini, F. Vizza, P. Frediani, J. A. Ramírez, *Organometallics* **1990**, *9*, 226–240.
- [14] R. M. Ward, A. S. Batsanov, J. A. K. Howard, T. B. Marder, *Inorg. Chim. Acta* **2006**, *359*, 3671–3676.
- [15] B. Stempfle, O. Gevert, H. Werner, *J. Organomet. Chem.* **2003**, *681*, 70–81.
- [16] a) C. J. Adams, N. G. Connelly, D. J. H. Emslie, O. D. Hayward, T. Manson, A. G. Orpen, P. H. Rieger, *Dalton Trans.* **2003**, 2835–2845; b) A. F. Hill, A. J. P. White, D. J. Williams, J. D. E. T. Wilton-Ely, *Organometallics* **1998**, *17*, 3152–3154.
- [17] a) H. Werner, O. Gevert, P. Haquette, *Organometallics* **1997**, *16*, 803–806; b) H. Werner, M. Schäfer, J. Wolf, K. Peters, H. G. von Schnering, *Angew. Chem.* **1995**, *107*, 213–215; *Angew. Chem. Int. Ed. Engl.* **1995**, *34*, 191–194; c) T. Rappert, O. Nürnberg, H. Werner, *Organometallics* **1993**, *12*, 1359–1364.
- [18] J. H. Barlow, M. G. Curl, D. R. Russell, G. R. Clark, *J. Organomet. Chem.* **1982**, *235*, 231–24.
- [19] F. Dahcheh, D. W. Stephan, *Organometallics* **2012**, *31*, 3222–3227.
- [20] K. Okamoto, Y. Omoto, H. Sano, K. Ohe, *Dalton Trans.* **2012**, *41*, 10926–10929.
- [21] A search in CCDB revealed some dinuclear complexes with at least one Rh(I) in an almost tetrahedral geometry, but showing, in addition, some type of metal-metal bond. Tetrahedral mononuclear complexes were not found. See for example: a) U. Herber, B. Weberndörfer, H. Werner, *Angew. Chem.* **1999**, *111*, 1707–1710; *Angew. Chem. Int. Ed.* **1999**, *38*, 1609–1613; b) P. Schwab, N. Mahr, J. Wolf, H. Werner, *Angew. Chem.* **1994**, *165*, 82–84; *Angew. Chem. Int. Ed.* **1994**, *33*, 97–99; c) R. A. Jones, T. C. Wright, J. L. Atwood, W. E. Hunter, *Organometallics* **1983**, *2*, 470–472.
- [22] See for example: a) C. Tejel, L. Asensio, M. P. del Río, B. de Bruin, J. A. López, M. A. Ciriano, *Eur. J. Inorg. Chem.* **2012**, 512–519; b) C. Tejel, M. P. del Río, L. Asensio, F. J. van den Bruele, M. A. Ciriano, N. Tschlis i Spithas, D. G. H. Hettterscheid, B. de Bruin, *Inorg. Chem.* **2011**, *50*, 7524–7534; c) C. Tejel, M. A. Ciriano, M. P. del Río, F. J. van den Bruele, D. G. H. Hettterscheid, N. Tschlis i Spithas, B. de Bruin, *J. Am. Chem. Soc.* **2008**, *130*, 5844–5845; d) C. Laporte, F. Breher, J. Geier, J. Harmer, A. Schweiger, H. Grützmacher, *Angew. Chem.* **2004**, *116*, 2621–2624; *Angew. Chem. Int. Ed.* **2004**, *43*, 2567–2570; e) B. Longato, R. Coppo, G. Pilloni, C. Corvaja, A. Toffoletti, G. Bandoli, *J. Organomet. Chem.* **2001**, *637*–639, 710–718; f) H. Schönberg, S. Boulmaâz, M. Wörle, L. Liesum, A. Schweiger, H. Grützmacher, *Angew. Chem.* **1998**, *110*, 1492–1494; *Angew. Chem. Int. Ed.* **1998**, *37*, 1423–1426; g) K. G. Moloy, J. L. Petersen, *J. Am. Chem. Soc.* **1995**, *117*, 7696–7710; h) A. S. C. Chan, H.-S. Shieh, J. R. Hill, *J. Organomet. Chem.* **1985**, *279*, 171–179; i) G. Pilloni, G. Zotti, M. Martelli, *Inorg. Chim. Acta* **1975**, *13*, 213–218.
- [23] See for example: a) H. Urtel, C. Meier, F. Rominger, P. Hofmann, *Organometallics* **2010**, *29*, 5496–5503; b) J. H. Rivers, R. A. Jones, *Chem. Commun.* **2010**, *46*, 4300–4302; c) E. Molinos, S. K. Brayshaw, G. Kociok-Köhn, A. S. Weller, *Dalton Trans.* **2007**, 4829–4844; d) P. Maire, A. Sreekanth, T. Büttner, J. Harmer, I. Gromov, H. Rügger, F. Breher, A. Schweiger, H. Grützmacher, *Angew. Chem.* **2006**, *118*, 3343–3347; *Angew. Chem. Int. Ed.* **2006**, *45*, 3265–3269; e) P. Maire, T. Büttner, F. Breher, P. Le Floch, H. Grützmacher, *Angew. Chem.* **2005**, *117*, 6477–6481; *Angew. Chem. Int. Ed.* **2005**, *44*, 6318–6323; f) Y. Nishihara, K. Nara, Y. Nishide, K. Osakada, *Dalton Trans.* **2004**, 1366–1375; g) V. Di Noto, G. Valle, B. Zarli, B. Longato, G. Pilloni, B. Corain, *Inorg. Chim. Acta* **1995**, *233*, 165–172; h) D. A. Hoic, W. M. Davis, G. C. Fu, *J. Am. Chem. Soc.* **1996**, *118*, 8176–8177; i) D. L. Thorn, R. L. Harlow, *Inorg. Chem.* **1990**, *29*, 2017–2019; j) M. J. Menu, G. Crocco, M. Dartiguenave, Y. Dartiguenave, G. Bertrand, *Organometallics* **1988**, *7*, 2231–2233; k) J. A. Kaduk, J. A. Ibers, *Inorg. Chem.* **1975**, *14*, 3070–3073.

- [24] D. Ostendorf, C. Landis, H. Grützmacher, *Angew. Chem.* **2006**, *118*, 5293–5297; *Angew. Chem. Int. Ed.* **2006**, *45*, 5169–5173.
- [25] A. M. Geer, A. Julián, J. A. López, M. A. Ciriano, C. Tejel, *Chem. Eur. J.* **2014**, *20*, 2732–2736.
- [26] C. Tejel, A. M. Geer, S. Jiménez, J. A. López, M. A. Ciriano, *Organometallics* **2012**, *31*, 2895–2906.
- [27] J. D. Feldman, J. C. Peters, T. D. Tilley, *Organometallics* **2002**, *21*, 4050–4084.
- [28] T. A. Albright, J. K. Burdett, M. H. Whangbo, *Orbital Interactions in Chemistry*, 2nd Edn.; Wiley: NJ, USA, 2013; p 478.
- [29] P. B. Baker, *Adv. Organomet. Chem.* **1996**, *40*, 45–115.
- [30] J. D. Feldman, J. C. Peters, T. D. Tilley, *Organometallics* **2002**, *21*, 4065–4075.
- [31] G. Marinelli, I. E. -I. Rachidi, W. E. Streib, O. Eisenstein, K. G. Caulton, *J. Am. Chem. Soc.* **1989**, *111*, 2346–2347.
- [32] B. J. Rappoli, M. R. Churchill, T. S. Janik, W. M. Rees, J. D. Atwood, *J. Am. Chem. Soc.* **1987**, *109*, 5145–5149.
- [33] B. Askevold, M. M. Khusniyarov, E. Herdtweck, K. Meyer, S. Schneider, *Angew. Chem.* **2010**, *122*, 7728–7731; *Angew. Chem. Int. Ed.* **2010**, *49*, 7566–7569 and references therein.
- [34] See for example: A. M. Geer, J. A. López, M. A. Ciriano, C. Tejel, *Organometallics* **2016**, *35*, 799–808.
- [35] A simple way of evaluating the electron-releasing character of a ligand for a specific complex is by comparison of the carbonyl stretching frequencies, $\nu(\text{CO})$ in related complexes. In this sense, comparison of the $\nu(\text{CO})$ values in the complexes $[\text{Mn}(\text{CO})_2(\text{L})\{\text{HC}(\text{PzMe}_2)_3\}]^+$ (L = PMe_3 , 1945, 1866 cm^{-1} ; CN^-Bu , 1963, 1896 cm^{-1}) indicates a more electron-releasing character for PMe_3 . See: A. J. Hallett, R. A. Baber, A. G. Orpen, B. D. Ward, *Dalton Trans.* **2011**, *40*, 9276–9283.
- [36] D. Balcells, E. Clot, O. Eisenstein, *Chem. Rev.* **2010**, *110*, 749–823.
- [37] B. M. Trost, J. T. Masters, *Chem. Soc. Rev.*, **2016**, *45*, 2212–2238.
- [38] C. J. Pell, O. V. Ozerov, *ACS Catal.* **2014**, *4*, 3470–3480 ([cat]: 1%, substrate: $p\text{-tolC}\equiv\text{CH}$, T: 80 °C, time: 3 h, conv.: 98%, *E/gem*-enyne: 69/29).
- [39] L. Rubio, R. Azpíroz, A. Di Giuseppe, V. Polo, R. Castarlenas, J. Pérez-Torrente, L. A. Oro, *Chem. Eur. J.* **2013**, *19*, 15304–15314 ([cat]: 5%, substrate: $\text{PhC}\equiv\text{CH}$, additive: py, T: 40 °C, time: 6 h, conv.: 99%, 92% *gem*-enyne).
- [40] W. Weng, C. Guo, R. Çelenligil-Çetin, B. M. Foxman, O. V. Ozerov, *Chem. Commun.* **2006**, 197–199 ([cat]: 0.5%, substrate: $\text{PhC}\equiv\text{CH}$, T: 100 °C, time: 8 h, conv.: 98%, 99% *E*-enyne).
- [41] a) H. M. Peng, J. Zhao, X. Li, *Adv. Synth. Catal.* **2009**, *351*, 1371–1377 ([cat]: 2.5%, substrate: $\text{TsNHCH}_2\text{C}\equiv\text{CH}$, T: 23 °C, time: 24 h, conv.: 99%, 83% *gem*-enyne); b) J. Ohshita, K. Furumori, A. Matsuguchi, M. Ishikawa, *J. Org. Chem.* **1990**, *55*, 3277–3280 ([cat]: 2%, substrate: $\text{PhC}\equiv\text{CH}$, T: 25 °C, time: 14 h, *E*-enyne: 20%, *gem*-enyne: 14%).
- [42] W. T. Boese, A. S. Goldman, *Organometallics* **1991**, *10*, 782–786 ([cat]: 2.5%, substrate: $\text{PhC}\equiv\text{CH}$, T: 25 °C, time: 14 h, 100% *gem*-enyne).
- [43] M. Schäfer, J. Wolf, H. Werner, *Organometallics* **2004**, *23*, 5713–5728 ([cat]: 1%, substrate: $\text{PhC}\equiv\text{CH}$, T = 40 °C, time: 4 h, conv.: 50%, *E/gem*-enyne: 70/30).
- [44] a) C. M. Storey, M. R. Gyton, R. E. Andrew, A. B. Chaplin, *Angew. Chem.* 10.1002/ange.201807028; *Angew. Chem. Int. Ed.* 10.1002/anie.201807028 (CNC-Me: [cat]: 5%, substrate: $\text{ArC}\equiv\text{CH}$, T: 25 °C, $t_{1/2}$: 4.2 h, conv.: > 90%, 100% *gem*-enyne); b) G. Kleinhaus, G. Guisado-Barrios, D. C. Liles, G. Bertrand, D. I. Bezuidenhout, *Chem. Commun.* **2016**, *52*, 3504–3507 ([cat]: 1%, substrate: 1-hexyne, additive: K_2CO_3 , T: 80 °C, time: > 1 h, conv.: 99%, 100% *gem*-enyne).
- [45] See for example: a) O. S. Morozov, A. F. Asachenko, D. V. Antonov, V. S. Kochurov, D. Yu. Paraschuk, M. S. Nechaev, *Adv. Synth. Catal.* **2014**, *356*, 2671–2678; b) G. Chandra Midya, B. Parasar, K. Dhara, J. Dash, *Org. Biomol. Chem.* **2014**, *12*, 1812–1822; c) J. S. Merol, F. T. Ladipo, *Polyhedron* **2014**, *70*, 125–132; d) B. Powala, C. Pietraszuk, *Catal. Lett.* **2014**, *144*, 413–418; e) O. V. Zatulochnaya, E. G. Gordeev, C. Jahier, V. P. Ananikov, V. Gevorgyan, *Chem. Eur. J.* **2014**, *20*, 9578–9588; f) S. Ventre, E. Derat, M. Amatore, C. Aubert, M. Petit, *Adv. Synth. Catal.* **2013**, *355*, 2584–2590.
- [46] E. Buxaderas, D. A. Alonso, C. Nájera, *RSC Adv.* **2014**, *4*, 46508–46512.
- [47] N. Gorgas, L. G. Alves, B. Stöger, A. M. Martins, L. F. Veiros, K. Kirchner, *J. Am. Chem. Soc.* **2017**, *139*, 8130–8133.
- [48] G. V. Oshovsky, B. Hessen, J. N. H. Reek, Bas de Bruin, *Organometallics* **2011**, *30*, 6067–6070.
- [49] a) J. Alós, T. Bolaño, M. A. Esteruelas, M. Oliván, E. Oñate, M. Valencia, *Inorg. Chem.* **2013**, *52*, 6199–6213; b) C. Jahier, O. V. Zatulochnaya, N. V. Zvyagintsev, V. P. Ananikov, V. Gevorgyan, *Org. Lett.* **2012**, *14*, 2846–2849; c) R. Ghosh, X. Zhang, P. Achord, T. J. Emge, K. K. Jespersen, A. I. S. Goldman, *J. Am. Chem. Soc.* **2007**, *129*, 853–866; d) M. Schäfer, J. Wolf, H. Werner, *Dalton Trans.* **2005**, 1468–1481; e) M. Schäfer, N. Mahr, J. Wolf, H. Werner, *Angew. Chem.* **1993**, *105*, 1377–1379; *Angew. Chem. Int. Ed. Engl.* **1993**, *32*, 1315–1318.
- [50] a) O. Torres, A. Roglans, A. Pla-Quintana, J. M. Luis, M. Solà, *J. Organomet. Chem.* **2014**, *768*, 15–22; b) M. Yamanaka, M. Morishima, Y. Shibata, S. Higashibayashi, H. Sakurai, *Organometallics* **2014**, *33*, 3060–3068; c) L. Orian, L. P. Wolters F. M. Bickelhaupt, *Chem. Eur. J.* **2013**, *19*, 13337–13347; d) M. Parera, A. Dachs M Solà, A. Pla-Quintana, A. Roglans, *Chem. Eur. J.* **2012**, *18*, 13097–13107; e) N. Agenet, V. Gandon, K. P. C. Vollhardt, M. Malacria, C. Aubert, *J. Am. Chem. Soc.* **2007**, *129*, 8860–8871.
- [51] N. E. Schore, *Chem. Rev.* **1988**, *88*, 1081–1119.
- [52] G. Bottari, L. L. Santos, C. M. Posadas, J. Campos, K. Mereiter, M. Paneque, *Chem. Eur. J.* **2016**, *22*, 13715–13723.
- [53] J. L. Herde, J. C. Lambert, C. V. Senoff *Inorg. Synth.* **1974**, *15*, 18–20.
- [54] M. A. Arthurs, J. Bickerton, S. R. Stobart, J. Wang *Organometallics*, **1998**, *17*, 2743–2750.
- [55] See supporting information for complete reference.
- [56] a) C. Lee, W. Yang, R. G. Parr, *Phys. Rev. B* **1988**, *37*, 785–789; b) A. D. Becke, *J. Chem. Phys.* **1993**, *98*, 1372–1377; c) A. D. Becke, *J. Chem. Phys.* **1993**, *98*, 5648–5652. (c) Grimme, S.; Antony, J.; Ehrlich, S.; Krieg, H. *J. Chem. Phys.* **2010**, *132*, 154104.
- [57] G. M. Sheldrick, SADABS, Bruker AXS, Madison, WI (USA), 1997.
- [58] G. M. Sheldrick, *Acta Cryst.* **2015**, *C71*, 3–8.
- [59] L. F. Farrugia, *J. Appl. Crystallogr.* **1999**, *32*, 837–838.

Entry for the Table of Contents (Please choose one layout)

Layout 2:

FULL PAPER



Ana M. Geer, Alejandro Julián, José A. López, Miguel A. Ciriano, and Cristina Tejel*

Page No. – Page No.

Pseudo-Tetrahedral Rhodium and Iridium Complexes: Catalytic Synthesis of E-enynes

Eighteen-electron pseudo-tetrahedral Rh(I) and Ir(I) complexes are generated with alkynes as four-electron donors. On addition of two-electron ligands the rhodium complexes undergo a C–H bond activation via pentacoordinate intermediates while these are the final products with iridium. Stoichiometric reactions with alkynes give new pseudo-tetrahedral rhodium complexes with η^2 -C≡C coordinated enynes while these reactions are catalytic with highly enhanced activity in MeCN.